Gas flaring and resultant air pollution

Fawole, Olusegun G.; Cai, X. M.; Mackenzie, A. R.

DOI:
10.1016/j.envpol.2016.05.075

Table of Content

Gas flaring and resultant air pollution: A review focusing on Black Carbon

Olusegun G. Fawole[1, 3], X. -M. Cai[1] and A. R. MacKenzie[1, 2]*

[1]School of Geography, Earth and Environmental Sciences, University of Birmingham, Edgbaston, Birmingham, B15 2TT, UK

[2]Birmingham Institute of Forest Research, University of Birmingham, Edgbaston, Birmingham, B15 2TT, UK

[3]Environmental Research Laboratory, Department of Physics, Obafemi Awolowo University, Ile-Ife, Nigeria 220005

*Corresponding author: a.r.mackenzie@bham.ac.uk

Abstract

Gas flaring is a prominent source of VOCs, CO, CO_2, SO_2, PAH, NO_X and soot (black carbon), all of which are important pollutants which interact, directly and indirectly, in the Earth's climatic processes. Globally, over 130 billion cubic metres of gas are flared annually. We review the contribution of gas flaring to air pollution on local, regional and global scales, with special emphasis on black carbon (BC, "soot"). The temporal and spatial characteristics of gas flaring distinguishes it from mobile combustion sources (transport), while the open-flame nature of gas flaring distinguishes it from industrial point-sources; the high temperature, flame control, and spatial compactness distinguishes gas flaring from both biomass burning and domestic fuel-use. All of these distinguishing factors influence the quantity and characteristics of BC production from gas flaring, so that it is important to consider this source separately in emissions inventories and environmental field studies. Estimate of the yield of pollutants from gas flaring have, to date, paid little or no attention to the emission of BC with the assumption often being made that flaring produces a smokeless flame. In gas flares, soot yield is known to depend on a number of factors, and there is a need

to develop emission estimates and modelling frameworks that take these factors into consideration. Hence, emission inventories, especially of the soot yield from gas flaring should give adequate consideration to the variation of fuel gas composition, and to combustion characteristics, which are strong determinants of the nature and quantity of pollutants emitted. The buoyant nature of gas flaring plume, often at temperatures in the range of 2000 K, coupled with the height of the stack enables some of the pollutants to escape further into the free troposphere aiding their long-range transport, which is often not well-captured by model studies.

Capsule Abstract

The review identified gaps in the estimation of emissions from the gas flaring process and argues for explicit recognition of gas flaring emissions in emission inventories and global models.

Keywords

Gas flaring; Oil and gas; Black Carbon; Incomplete combustion; Hydrocarbon; Emission factors

Variables used and their meanings

u_e	exit velocity of the flue gas (m s^{-1})
s	the air-fuel ratio
ρ_e, ρ_∞	the fuel gas and ambient densities respectively (kg m^{-3})
g	acceleration due to gravity (m s^{-2})
ΔT_f	mean peak flame temperature rise, K (taken as the difference between the adiabatic flame temperature and the ambient temperature)
d_e	burner diameter (m)
υ_o	kinematic viscosity of the gas-air mixture (m^2 s^{-1})
L	characteristic flame length (m)
$\dot{m}_o$	mass flux of the flue gas at the burner exit ($kgm^{-2}s^{-1}$)
f_s	stoichiometric mixture fraction
ϕ	equivalence ratio
T_∞	ambient temperature

1 Introduction

1.1 Motivation

Humans need energy to drive their technology: and hence, make life pleasurable and worth living. Different forms of energy are in use and new ones are developed in order to meet the increasing needs of society (MacKay, 2008). This quest for dependable, affordable and environmentally benign energy sources has occurred throughout human history; for the last century or so, crude oil has been the focus of world energy. In 2011, crude oil was estimated to provide 52.8 % of the world's energy (13113 Mtoe); with oil and natural gas accounting for 31.5 % and 21.3 % respectively (IEA, 2013).

Human reliance on oil and gas as an energy source is not without its attendant impact on the environment. During production, detrimental impacts on the environment (air, water and soil) include: oil spills and leakages; venting; sludge disposal; and flaring (Almanza et al., 2012; Osuji and Adesiyan, 2005; Osuji and Onojake, 2004; Sonibare et al., 2010). The post-production impact of oil and gas on the environment is also a major source of concern, but is not the subject of this review.

Gas flaring is often a routine daily activity in oil fields around the world, particularly in oil-rich regions of the world where the infrastructure to capture, store and utilise the gas produced is not available. Flaring is most often associated with Nigeria and the Russian Arctic, but it does still occur in more developed economies: the North Dakota Bakken shale region, for instance (see, e.g., http://www.eia.gov/todayinenergy/detail.cfm?id=23752, last accessed on 29 January 2016). Despite several calls by international bodies such as the World Bank's Global Gas Flaring Reduction (GGFR) initiative, the volume of gas flared globally appears to have plateaued at around 130 billion cubic metres (bcm) since 2008, or may even have increased (see section 1.4, below). According to GGFR (2013), there was an increase of 2 bcm in the volume of gas flared in 2011 compared to the previous year. The latest in this series of initiatives by the World Bank - Zero Routine Flaring by 2030 - was launched by the Secretary-General of the United Nations, Ban Ki-Moon and World Bank's President, Jim Yong Kim, in May, 2015 (see http://www.worldbank.org/en/programs/zero-routine-flaring-by-2030, last accessed on January 29, 2016).

Gas flaring, a prominent source of black carbon (BC) and other pollutants, has been ignored or underestimated in emission inventories and models, as a result of which models are struggling to predict measurements of BC in regions of intense gas flaring. The intensity of gas flaring and specifics of atmospheric transport can combine to enhance the role of gas flaring emissions over very large areas (e.g., the Arctic) (Stohl et al., 2013). Presently, treatment of emissions from gas flaring is rather rudimentary in most global emission inventories. As at 2015, to the best of our knowledge, only two global pollutants inventories explicitly accounted for emissions from gas flaring (see section 4.5).

Gas flaring is classified as a miscellaneous BC-rich source, a group which includes aviation and shipping which together contribute about 9 % to global BC emission (Bond et al., 2013). Gas flaring is a very different type of combustion compared to other BC sources in this category; gas flaring is characterised by either fuel-regulated or oxidant-regulated open-fire (see below) resulting in flames that can be 8-10 metres in length, with flame temperature as high as 2000K. Gas flaring is a year-round activity in most of the intensive flaring regions of the world, and so differs from transport sources in being stationary and differs from other stationary sources (e.g. cooking and biomass burning) by being relatively constant in time. The GAINS (Greenhouse gas Air pollution INteractions and Synergies) model estimated that gas flaring contributes about 4 % of total anthropogenic BC emissions, majority of which are from the leading gas-flaring nations; Russia, Nigeria, and countries in the Middle East (Bond et al., 2013; Stohl et al., 2013). Gas flaring is estimated to contribute 260 Gg to global BC estimates annually (Bond et al., 2013), while in Russia, it is estimated to have the largest contribution of 36.2 % to anthropogenic BC emission (Huang et al., 2015). From a 3-year model simulation, more than 40% of annual mean BC near the surface in the Arctic is estimated to be contribution from gas flaring (Stohl et al., 2013).

Considering the small number of nations that still flare gas, a contribution of 4 % to global BC represents a significant skew in the global apportionment of BC emissions. On a regional scale, the contribution of this 'overlooked' source of ambient aerosol loading is likely to be significant.

1.2 Review summary

For this review, we have collated previous studies (1984-2015) on gas flaring and its contributions to ambient aerosol loadings. This review is the first to cover virtually every aspects of gas flaring (process, trends, chemistry, flame dynamics and environmental impact). The review starts with a brief assessment of the level and distribution of oil and gas reserves around continents of the world. Compositional variation of the natural gas flared and their thermodynamic properties are discussed because they are likely to have significant impact on pollutant emission rates and overall amount. Next, we provide a discussion of the temporal and geographical trends in gas flaring, including brief comments about how weather conditions in regions where gas flaring is common will impact near-field dispersion and long-range transport. This is followed by a broad discussion of the gas flaring process itself; highlighting how engineering and technology decisions impact on the emission of air pollutants. Finally, several techniques used to estimate emissions from gas flaring are discussed. Throughout this review, special attention is paid to soot (i.e. carbonaceous aerosol predominantly composed of BC) emission from gas flaring because of the now known contribution of BC to global warming and the apparent neglect of the contribution of gas flaring to ambient air aerosol loadings in inventories and global models.

1.3 Global oil and gas reserves

World-proven natural gas and oil reserves at the end of 2012 stood at 187.3 and 1668.9 trillion cubic metres (tcm) respectively, sufficient to meet 55.7 years of global production (BP, 2013). The distribution of these reserves among regions of the world is shown in Figures 1(a) and (b). The natural gas collected during the exploration of crude oil from the Earth's crust can be a very good source of fuel; transported in pipes for industrial or domestic use and also recycled back into the processing operation (Davoudi et al., 2013; Elvidge et al., 2009).

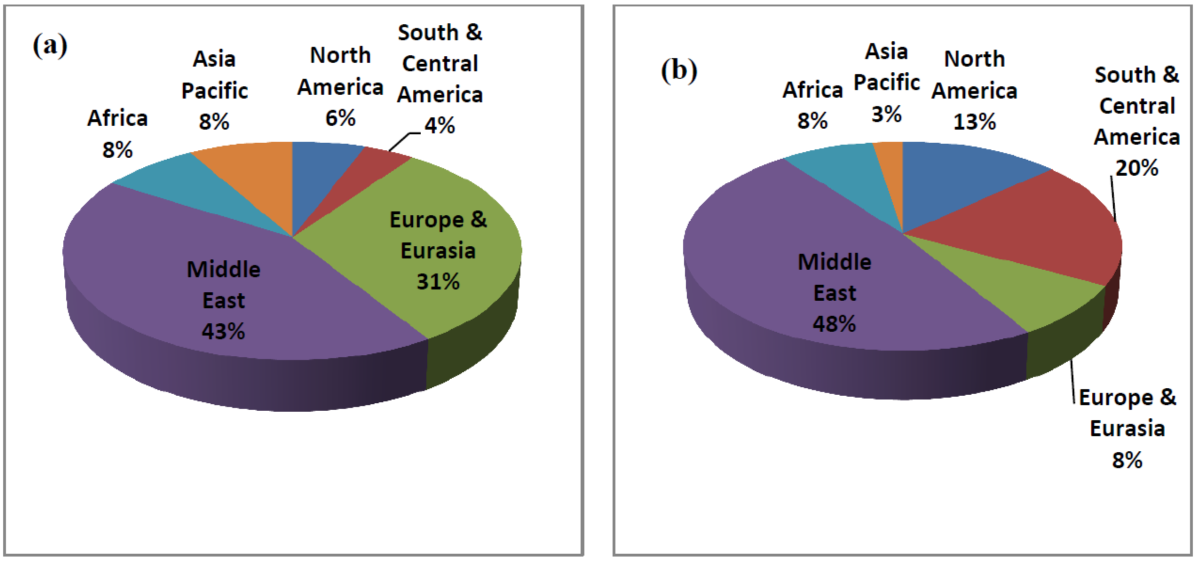

Figure 1: (a) The distribution of world natural gas reserves (b): The distribution of world oil reserves (adapted from BP (2013).

In developing countries and oil-rich regions where the technology, infrastructure, and market structure to put all of the natural gas to meaningful use are not available or inadequate, the excess natural gas then becomes a waste stream and is flared or vented. Gas flaring has been termed 'gross waste' by the World Bank's initiative against gas flaring (Global gas flaring reduction: GGFR), because flaring represents direct injection of fossil carbon into the atmosphere without capture and utilization of the heat produced by combustion.

1.4 Temporal and geographical trends in gas flaring

The all-time peak of volume of gas flared, 172 bcm, was in 2005 (Elvidge et al., 2009). Figure 2(a) shows the quantity of natural gas produced by the top 10 oil producing nations of the world between 2000 and 2011, and for comparison, Figure 2(b) shows the estimated quantity of gas flared by these major oil producing nations during the same period of time. The estimated volume of gas flared globally in 2012 is also shown in Figure 2(b): the 2012 data is obtained from Elvidge et al. (2015). Data for the plots in figure 2(a) and (b) are from IEA (2012) and GGFR (2012), respectively. Between 2008 and 2011, there was no significant decrease in the amount of natural gas flared. In fact, there was a slight increase between 2010 and 2011. According to (BP, 2015), the production excludes the quantity flared or recycled. Therefore, total fossil fuel extracted and ultimately released to the environment is the sum of the production and quantity flared.

Figure 3 gives the temporal variation of the fraction of total gas extracted that is flared between 2000 and 2011. Nigeria, Libya and Kazakhstan still flare a sizeable amount of their total production. As at 2011, Nigeria and Libya flared about 30 % of their total gas extracted while Kazakhstan flares about 15 %. The 30 % (15.2 bcm) flared by Nigeria is more than twice Libya's total gas extracted (6.3 bcm) for the same period. Russia and Nigeria together account for about 35 % of the gas flared globally (Elvidge et al., 2009). Although the fraction of gas flared is decreasing for most countries and for the largest emitters, several countries show flat or increasing fractions of gas flared. The estimated quantity of natural gas flared in the US and Canada, as shown in Figure 2b, are just for the off-shore flaring which is presumably responsible for the very low quantities recorded. After 2006, there is a factor of 22 and 10 increase in flaring from USA and Canada, respectively, resulting, presumably, from increased exploitation of unconventional hydrocarbon reservoirs ('fracking').

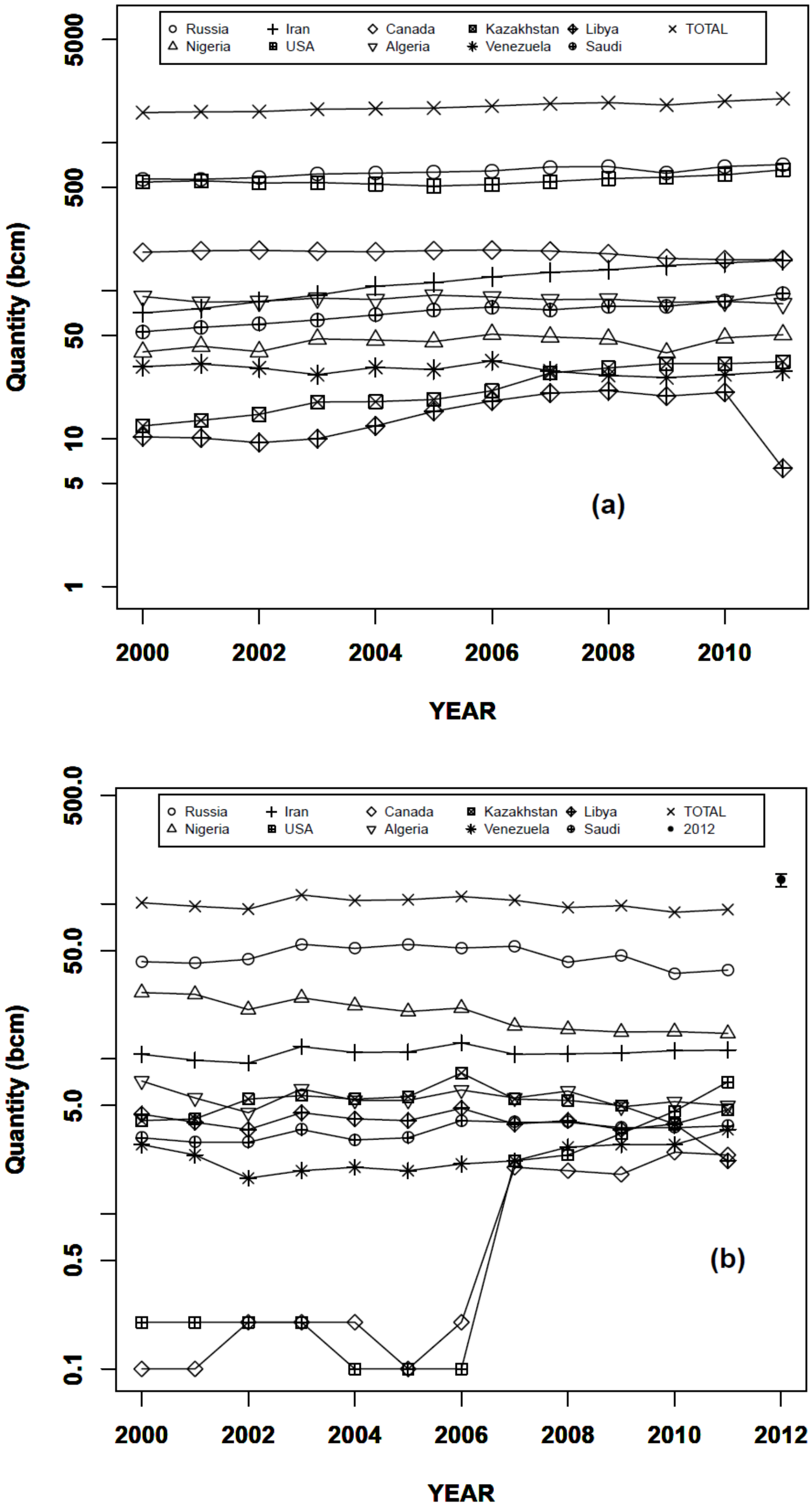

Figure 2: Trend of natural gas (a) production and (b) flaring in major oil producing nations between 2000 and 2011 (adapted from IEA (2012) and (GGFR, 2012) respectively).

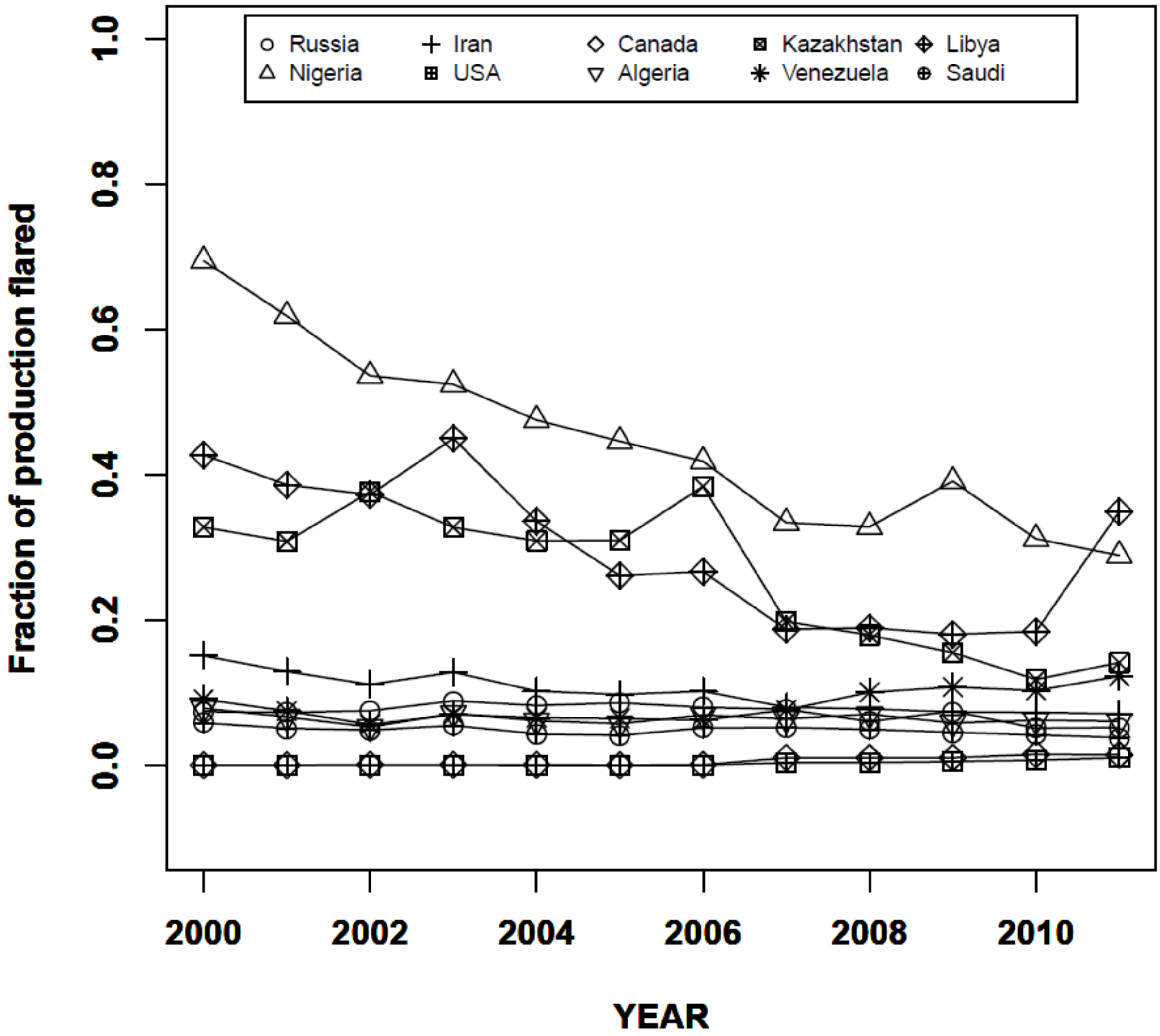

Figure 3: Trend of quantity flared compared to total production (data from Figure 2)

Table 1 gives the estimates, from satellite data, of the quantity of gas flaring by the top 20 gas flaring nations of the world in 2008 and a brief summary of the climatic conditions of the region based on the Köppen climate classification (see, e.g., Holden (2005))

Figure 4, reproduced, with permission, from Casadio et al. (2012), shows the global geographic distribution of gas flaring sites obtained by remote sensing techniques. In Africa, the flaring spots are clustered around the North - Algeria, Libya and Egypt - as well as around the Atlantic Ocean especially the Niger Delta area of Nigeria. In Europe, they are around Russia and Kazakhstan, and Iran, Iraq, Kuwait, and Saudi Arabia in the Middle East. Satellite remote sensing not only gives a general picture of the spatial distribution of flares, but also a gross estimation globally at national levels.

Table 1: Year 2008 estimated gas flared by top 20 gas flaring nations with an estimated error of ±2.11bcm.

Rank	Country	Gas Flared (bcm)	Regional Climate	Comments*
1	Russia	40.5	(Dfa, Dfb, Dwa, Dwb), (Dfc,Dfd, Dwc, Dwd) and ET	peri-Arctic emissions; pole-ward atmospheric flow around Tibetan anticyclone in northern hemisphere winter
2	Nigeria	15.1	Am and Aw	Tropical monsoon and trade-wind littoral and tropical wet and dry climate resulting from West African monsoon winds that changes direction with season; climatic condition is controlled by trade wind and movement of the ITCZ
3	Iran	10.4	Bwh	Tropical and subtropical desert climate characterised by large diurnal temperature range. Deep turbulent boundary layer during the day; shallow stable boundary layer at night. Large-scale subsidence (descending branch of the Hadley circulation) above the boundary layer.
4	Iraq	7.0	Bsh	Mid-latitude steppe and desert climate characterised by semiarid annual rainfall distribution
5	Algeria	5.5	Bwh	As for Iran
6	Kazakhstan	5.2	Bwk	Mid-latitude arid wet and dry climate
7	Libya	3.8	Bwh	As for Iran
8	Saudi Arabia	3.5	Bwh	As for Iran
9	Angola	3.1	Cwa	Humid subtropical climate; equatorward and poleward circulation during winter and summer respectively cause changes in the movement of air masses from the cold polar and warm tropics within this climate.
10	Qatar	3.0	Bwh	As for Iran
11	Uzbekistan	2.7	Csa	Mediterranean climate; it is controlled by the variation between subtropical high in summer and

				polar westerlies in winter
12	Mexico	2.6	Af, Aw, Bsh, Bsk, Bwh, Cwa, Cwb, Cfa, Cfb	Complex climatic condition; two tropical, two dry and three temperate climates
13	Venezuela	2.6	Aw	Tropical wet-dry climate
14	Indonesia	2.3	Aw, Am	As for Nigeria (see comment above)
15	USA	2.3	Bsk, Bsh, Bwk, Csa, Csb, Af	Mediterranean/dry summer subtropical climate characterised by moist winter and hot dry summer; subtropical anticyclones are key factor that control this climate
16	China	2.3	Cfa, Cwa	Humid subtropical climate; during winter the climate is influenced by the Siberian cold and during summer there is an inflow warm of air from the west
17	Oman	1.9	Bwh	As for Iran
18	Malaysia	1.9	Af	Tropical rainforest characterised by constant high temperatures and evenly distributed high precipitation; controlled by movement of the ITCZ and rising air along trade wind coast. Strongly affected by el Nino Southern Oscillation
19	Canada	1.8	Dfb, Dfd, Dsc, Af	As for Russia (see above)
20	Kuwait	1.8	Bwh	As for Iran
	TOTAL	119.3		

Source: Quantity of gas flared is obtained from Elvidge et al. (2009). *See Holden (2005)

Elvidge et al. (2015), using data collected by National Aeronautics and Space Administration/National Oceanic and Atmospheric Administration Visible Infrared Imaging Radiometer Suite (VIIRS), identified more than 7000 active flare globally in 2012: the bulk of which were found in the upstream sector of the oil and gas industries. In 2012, the estimated volume of gas flared globally is 143±13.6 bcm (Elvidge et al., 2015). Compared to 119.3±2.11 bcm estimated for 2008 (Elvidge et al., 2009), this is an increment of about 20 % in the central tendencies of the estimates for both years and is well outside the combined uncertainty bounds of both estimates. An increment of about 20 % over four years, stands in stark contrast to the decrease anticipated as a result of the World Bank's Global Gas Flaring

Reduction (GGFR) initiative. A new dimension to the problem is the inclusion of three new countries – India, Egypt and Turkmenistan - in the list of top 20 gas flaring countries.

The geographical location of the sources of gas flaring emissions (as monitored from space, see Figure 4), the atmospheric behaviour of emitted pollutants, and the pollutant “matrix” from other sources into which emission are made, determine to a large extent the effect gas flaring emissions will have on regional pollution loadings and on climate. BC emissions in the peri-Arctic and West African Monsoon (WAM) regions have the potential to interact with regional radiative energy budgets and atmospheric circulations, leading to impacts on their respective regional climates. Gas flaring emissions in the tropics, especially the WAM and South Asian Monsoon (SAM), could have significant regional impact as a result of the intense convective activities and cloud formation in these regions.

Monsoon circulations are characterised by large-scale seasonal reversals of wind regimes. Regions often referred to as ‘monsoonal’ include tropical and near-tropical regions which experience a summer rainfall maximum and most of these regions have a double rainfall maximum (Barry and Chorley, 2009). The annual climatic regime over West Africa has many similarities to that of South Asia. Both are characterised by surface air-flow which is determined by the position of the leading edge of a monsoon trough. Winds are south-westerly to the south of the trough and north-easterly to the North. The lack of a large mountain range in the north of West Africa strongly enhances the northward advance of the WAM compared to its South Asian counterpart. The position of the leading edge of the WAM trough may oscillate greatly from day-to-day through several degrees of latitude (Barry and Chorley, 2009). In the WAM, deep convection occurs in organised systems known as Mesoscale Convective Systems (MCS) (Mari et al., 2011; Mathon and Laurent, 2001). Deep convection in the tropics associated with the ITCZ is responsible for intense mixing, venting of the atmospheric boundary layer, and long-range transport of aerosol (Law et al., 2010; Reeves et al., 2010; Sultan and Janicot, 2003).

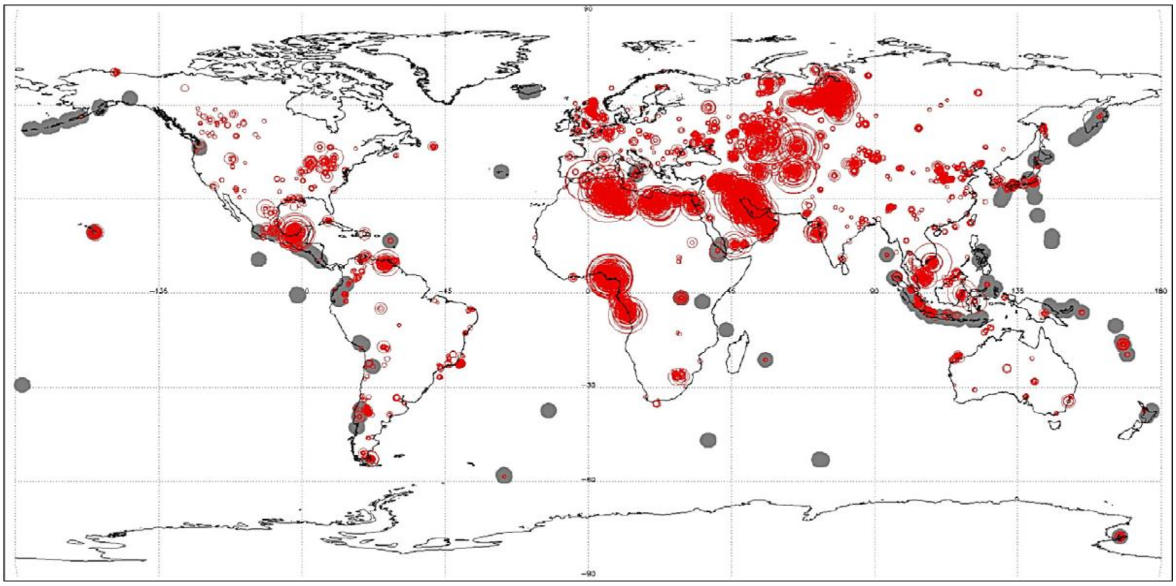

Figure 4: Flaring hot spot sites (1991-2009) as monitored from space are indicated as red spots while grey spots represent position of active volcanoes during the same period Casadio et al. (2012).

2 Oil and Gas Production

2.1 Exploration and exploitation

Oil exploration can be a very complex and capital intensive process as oil deposits are often located in reservoirs buried far into the Earth. These locations can be in very remote and inhospitable parts of the Earth and can be either on- or off-shore. The multi-staged process of exploration, exploitation and processing of crude oil in its raw form from the Earth's crust can be broadly divided into upstream, midstream and downstream. Environmental contaminants are expelled into the ambient environment - soil, air and water - at different stages of the process. Crude oil is found in reservoirs which also contain gas. This gas is known as "*associated natural gas*", and it is separated from the crude oil at a Flow Station. Natural gas includes both "*non-associated*" gas originating from fields producing only gaseous hydrocarbons, and "associated" gas produced in association with crude oil (IEA, 2012). Natural gas comprises mainly hydrocarbons, predominantly short-chained alkanes. At the separation stage, some of the natural gas is captured for domestic and industrial use while the rest is disposed of, usually by *flaring* in open flames. Below, we will use the term ‘fuel gas’ to refer to natural gas that is flared. The quantity of contaminants expelled at this stage of processing depends on the technology employed, quantity of crude oil processed, flare geometry and design, prevailing meteorological conditions and the composition of the flared gas (E & P Forum, 1994; Ismail and Umukoro, 2014; Johnson and Coderre, 2011; Obanijesu et al., 2009; Ouf et al., 2008; Sonibare and Akeredolu, 2004; Talebi et al., 2014).

Oil and gas are produced in many wells in different parts of the world at rates varying from 50 m^3 to 700 m^3 per day. As a result of the diverse nature of the geological features of the area where these explorations take place, the composition of oil and gas varies from one station to another.

2.2 Composition of natural gas

The composition of natural gas from 10 stations from around the world is given in Table 2. Fuel gas is a combination of C_1 to C_{7+} hydrocarbons which are predominantly alkanes. A typical fuel gas sample contains CH_4, C_2H_6, C_3H_8, n-C_4H_{10}, i-C_4H_{10}, n-C_5H_{12}, i-C_5H_{12}, C_6H_{14}, C_7H_{16}, H_2S, CO_2 and N_2, where ‘n’ and ‘i’ stand for ‘normal’ i.e., straight chained, ‘iso’ or branched-chained alkanes, respectively. The separation of gas and liquid is not perfect at the Flow Stations and as such trace amounts of liquid can occur in the gas stream, enhancing the abundance of higher molecular weight alkanes in the fuel gas.

Table 2: Composition (in mole %) and Some Properties of Fuel Gas from Field Stations and Literature.

Composition	**Flow Stations**										**Lab-based**	
	1	**2**	**3**	**4**	**5**	**6**	**7**	**8**	**9**	**10**	**A**	**B**
$\mathbf{CH_4}$	74.3	79.85	56.9	55.5	82.23	78.41	68.14	68.42	72.32	69.58	85.24	74.54
$\mathbf{C_2H_6}$	14.0	11.54	21.2	18.0	2.38	5.68	14.22	7.65	2.41	0.25	7.06	12.17
$\mathbf{C_3H_8}$	5.8	2.25	6.0	9.8	4.24	0.23	10.27	11.27	6.24	12.54	3.11	5.37
$\mathbf{nC_4H_{10}}$	2.0	2.58	3.7	4.5	0.94	0.70	3.23	4.39	8.12	2.35	1.44	2.49
$\mathbf{iC_4H_{10}}$	-	0.14	-	-	5.12	4.12	2.38	4.42	5.12	5.12	-	-
$\mathbf{nC_5H_{12}}$	0.9	3.24	1.6	1.6	2.25	9.12	0.75	0.94	3.14	5.20	-	-
$\mathbf{iC_5H_{12}}$	-	-	-	-	2.14	0.25	1.01	1.55	2.48	2.54	-	-
$\mathbf{C_6H_{14}}$	-	0.14	-	-	0.25	0.23	-	0.18	0.15	1.97	-	-
$\mathbf{N_2}$	2.9	0.1	-	0.2	-	0.05	-	0.16	-	0.24	1.24	2.15
$\mathbf{CO_2}$	-	0.16	7.1	8.9	0.45	1.21	-	1.02	-	0.21	1.91	3.28
$\mathbf{H_2S}$	0.1	-	3.5	1.5	-	-	-	-	0.02	-	-	-
***C:H**	0.2659	0.2715	0.2569	0.2602	0.2730	0.2751	0.2860	0.2852	0.2893	0.2924	0.2541	0.2570
***Molar mass (g mol^{-1})**	21.4	21.4	25.8	26.9	22.9	24.7	24.3	25.8	27.0	28.6	19.2	21.5
***Molar mass (g mol^{-1}) without CO_2 and N_2**	20.5	21.3	22.7	22.9	22.7	24.1	24.3	25.3	27.0	28.4	18.0	19.4
***HHV (MJ m^{-3})**	44.8	46.4	47.8	48.7	49.1	52.0	52.2	54.2	57.2	60.3	39.8	42.5

2 and 5 – 10 are adapted from Sonibare and Akeredolu (2004), 1, 3 and 4 from Ismail and Umukoro (2014) and lab-based (A&B) from McEwen and Johnson (2012)

Compositions 1, 3 and 4 are from Saudi Arabia, Kuwait and Iraq respectively while 2 and 5 - 10 are from different flow stations in Nigeria.

C:H = mass-weighted carbon to hydrogen ratio

* evaluated in this work

2.3 Thermodynamic properties of varying fuel gas compositions

The higher heating value (HHV) is the total enthalpy of the complete combustion reaction for the gas mixture, plus the heat of condensation of the water produced during combustion; lower heating value (LHV) is the total enthalpy of the complete combustion when water remains present in its gaseous form only (Flagan and Seinfeld, 2012). The Volumetric heating value (VHV), measured in kJ mol^{-1}, usually refer to the HHV unless otherwise stated. In gas flaring, HHV, calculable using data from standard thermodynamic tables, defines the total amount of energy available to provide buoyancy to the flare. Buoyancy is an important parameter in determining the dispersion of flare emissions (Beychok, 1994; Leahey and Davies, 1984). The heat content of a fuel gas depends on its molar mass and by extension the density of the fuel. Figure 5 presents the best fit line relating HHV to the molar mass of the fuel gases from the Flow Stations given in Table 2. This plot shows the extent of dependence of HHV on the molar mass, and hence, density of the fuel gas. These properties of the fuel gas, varies with the fuel composition. Note that the HHV values for the laboratory flares in Table 1 are lower that the HHV for the Flow Station fuel gases.

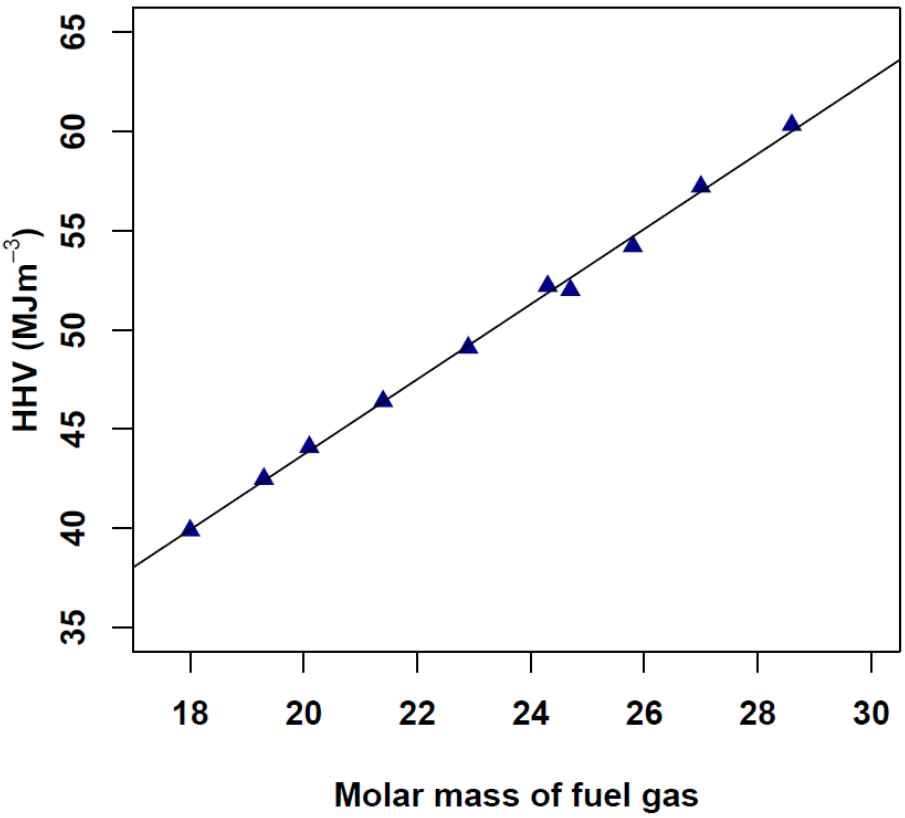

Figure 5: Higher heating value (HHV) as a function of molar mass of fuel gas for the Flow Station data reported in Table 1.

3 Overview of the gas flaring processes

Gas flaring is carried out with the aim to convert its hydrocarbon content, especially methane, to products that are less hazardous to the immediate vicinity of the flare site. Gas flaring is classified as a stationary combustion source for the purpose of air pollution regulation (USEPA, 2008). The combustion process involves the rapid oxidation of the fuel gas with the release of heat, gaseous and particulate pollutants, whose nature and quantity depend on the amount and composition of gas fuel burned, the combustion characteristics as well as the flare geometry and design (Ouf et al., 2008; Torres et al., 2012a).

Gas flaring may be categorized as *emergency*, *process* and *production* flaring depending on the basis of the flaring (Johnson and Coderre, 2011). *Emergency flaring* is unplanned: it is carried out at large facilities for safety purposes for a short duration of time. During emergency flaring, a large volume of gas is disposed of quickly and, hence, the flow rate of the fuel gas is very high. *Process flaring* is an intermittent disposal of unwanted gas that may last for a few hours or a couple of days at often low flow rate. It occurs during well-testing as well as start-up and shutdown of process units. *Production flaring* may occur continuously for years as long as the oil is being explored and exploited. The flow rate can be very high at particular times especially during the initial development of a gas well (Johnson and Coderre, 2011). As a result of the length of time involved, which can be years, and the flow rate of the gas flared, production flaring is the major process of concern for regional and global pollution, including interaction with climate.

3.1 Gas flaring emission and its environmental impact

Gas flaring is the process of disposing of gas (referred to as fuel gas in this review), by combustion in an open flame in the open atmosphere, using a burner tip designed specifically for that purpose, in the course of routine oil and gas production operations (McEwen and Johnson, 2012; OGP, 2000; Stone et al., 1992). Gas flaring is a source of greenhouse gases, precursor gases, VOCs, polycyclic aromatic hydrocarbon (PAH) and particulate matter (PM) in the form of soot (Ana et al., 2012; Johnson et al., 2013; McEwen and Johnson, 2012; USEPA, 2011; USEPA, 2012). These pollutants have been identified to have serious detrimental impact on animals, vegetation and human (Burney and Ramanathan, 2014; Dung et al., 2008; Pope III et al., 2002; USEPA, 2010). The *soot* emitted from the combustion of natural gas is predominantly *black carbon (BC)* (Johnson et al., 2013; Smith and Chughtai, 1995).

BC is a strong climate forcer and plays a prominent role in the nature of the Earth's climate because of its ability to absorb solar radiation, and hence, to result in a changed vertical gradient of warming by incoming solar radiation (Ramana et al., 2010; Ramanathan and Carmichael, 2008). It also affects cloud processes as well as decreasing surface albedo on ice and snow causing them to melt faster (IPCC, 2007). It can be short-lived in the atmosphere, as it is removed from the atmosphere by dry and wet deposition (although insoluble in water, it is wettable, particularly when 'aged' by atmospheric oxidation). When mixed with other aerosol components in the atmosphere, BC can affect the climate for longer as its residence time is increased in that state (Bond et al., 2013; Flanner et al., 2007; Quinn et al., 2008; Ramana et al., 2010). Within current estimated uncertainties, BC is the second highest contributor to global warming just after CO_2 (IPCC, 2007), and also the main light-absorbing component of atmospheric aerosols (Bond et al., 2013; Chung and Seinfeld, 2005; Jacobson, 2002; Ramanathan and Carmichael, 2008; Seinfeld, 2008).

The radiative forcing capacity of a cloud of aerosol particles depends on the ratio of the BC to other components in the cloud (Ramana et al., 2010). The ubiquitous nature of BC coupled with its several effects on the Earth's climate makes the study of its sources and emission rates important. If adequate measures are put in place to reduce BC emission, short-term reduction of radiative forcing can be achieved in the Arctic and other oil rich regions of the world (Arctic Council, 2013; Feichter and Stier, 2012; Tripathi et al., 2005).

Studies have shown that the contributions from oil and gas processing, especially gas flares, to air pollution have been severely underestimated (Edwards et al., 2013; Johansson et al., 2014; Schultz, 2014; Stohl et al., 2013). This is arguably due to the fact that emission factors (EF) often used to estimate the emissions of pollutants from the oil and gas sector, especially gas flaring, are too general and independent of site specifics such as fuel composition and combustion characteristics. There is a pressing research need for more measurements and development of EFs estimates that vary with the fuel gas composition and combustion characteristics.

At the local scale, ground-level measurements within one kilometre downwind of the flaring sites have indicated an elevated concentration of particulate and gaseous pollutants (Edwards et al., 2013; Obanijesu et al., 2009; Sonibare et al., 2010). Likewise, on a regional scale, flight campaign during ACCESS (Arctic Climate Change Economy and Society) around oil and gas installations in Heidrun, Norway reported elevated concentrations of NO, SO_2 and CO in the lower troposphere (Roiger et al., 2015).

NO_X ($NO+NO_2$), SO_2, CO_2, CO and unburned hydrocarbon are the major pollutant constituents of gas flaring plumes (USEPA, 1995). The low amount of the nitrogen and sulphur content of the fuel gas notwithstanding, the NO_X and SO_2 emission from gas flaring remain significant because the ambient background level of both pollutants are usually low. Hence, gas flaring can substantially enhance the local concentrations of these pollutants. Complete combustion is often not achieved in most flaring conditions (Leahey et al., 2001). During incomplete combustion, methane (CH_4) and other unburned components of the fuel gas are given off and some fuel components are partially oxidized to CO and soot rather than completely oxidised to CO_2 (RTI, 2011; Strosher, 2000; Villasenor et al., 2003). Equations 1a and b, respectively, give simplified equations for the 'ideal' complete and partial oxidation of the fuel gas. In equation (1b), '*rC'* denotes soot production, 'vO_2' excess oxygen in the case of fuel-lean combustion and 'C_aH_b' are PAH and other semi-volatile organics resulting from the pyrolysis of hydrocarbons in the fuel gas. The value of *m* in equation (1b) determines a fuel-lean (over-fired; m > x + y/4) or fuel-rich (under-fired; m < x + y/4) combustion process. The level of combustion (oxidation) of the fuel gas is dependent on a number of factors: the nature of the flame during combustion, the level of mixing of the gas and air in the reaction zone, the amount of oxidant (oxygen) available, the VHV of the fuel gas and the prevailing condition of the ambient wind (Stone et al., 1992). Flare design and geometry are also key determinants of the level of combustion of the fuel gas.

$$C_xH_y + \left(x + \frac{y}{4}\right) O_2 \rightarrow xCO_2 + \frac{y}{2} H_2O \quad \text{(1a)}$$

$$C_xH_y + m\,O_2 \rightarrow pCO_2 + qCO + rC + vO_2 + fH_2O + \sum_{a,b} d_{a,b}\,C_aH_b \quad \ldots\ldots\ldots\ldots \quad (1b)$$

For ‘ideal’ complete combustion, the oxidation of the hydrocarbon yields carbon dioxide and water only (equation 1a), while the oxidation of the sulphur (as H_2S) and nitrogen content of the fuel gas gives SO_2 and NO_X respectively. In gas flaring, NO_X is produced by thermal cracking of the nitrogen content of the fuel gas and entrained atmospheric nitrogen. The amount of carbon-containing emission (CO_2, CO, C_aH_b, and BC) given off depends on the molar mass of non-CO_2 carbon per mole of the fuel gas (cf. Table 2). Smoking of a gas flare does not necessarily imply that the combustion process is highly inefficient; because a small amount of soot can absorb and scatter perceptible amounts of visible light, a flare with a combustion efficiency of 99 % could still smoke visibly (Castineira and Edgar, 2006).

3.2 Emissions measurements around real-world gas flaring sites

Few data of pollutants measurement around gas flaring sites are publicly available. Data from the ACCESS aircraft campaign experiment in the Arctic (Norway) and a couple of ground-based in-situ measurements in Nigeria and the US show significant contributions from gas flaring to ambient air concentrations of these pollutants.

In-situ ground measurements of air pollutants around typical oil and gas facilities where varying degrees of gas flaring take place have been undertaken in the US (Edwards et al., 2013; Edwards et al., 2014; Johansson et al., 2014), Mexico (Villasenor et al., 2003), Norway (Roiger et al., 2015) and, Nigeria (Ana et al., 2012; Nwaichi and Uzazobona, 2011; Obanijesu et al., 2009; Sonibare et al., 2010). Continuous noise levels higher than the WHO limit of 70 dB were also observed around some gas flaring sites in Nigeria (Abdulkareem and Odigure, 2006; Avwiri and Nte, 2004).

A 4-month sampling of three air pollutants (SO_2, CO and NO_2) around six flow stations in the Niger Delta area of Nigeria was undertaken by Obanijesu et al. (2009) and Sonibare et al.

(2010). The measurements were made at 60, 200 and 500 m downwind of the flaring sites. Although to a varying degree depending on the capacity of the station, gas flaring is a prominent daily activity within the stations. Mean pollutants measurements around the six flow stations are shown in Figures 6(a), (b) and (c). The variation bar on the bar-plots shows the standard deviation of the measurements over the four-month period. The nature and extent of dispersion of pollutants from a stationary source depend on the local meteorology and topography of the area. As shown in Figures 6(a)-(c), the trend of the measurements from the flaring sites are similar to observations from dispersion model studies where concentrations of pollutants decreases exponentially with distance from the source (Hodgson et al., 2007). Site 4 is the only place where a significant deviation from this trend, especially for CO and NO_2, was observed, suggesting the likelihood of contributions from other source(s).

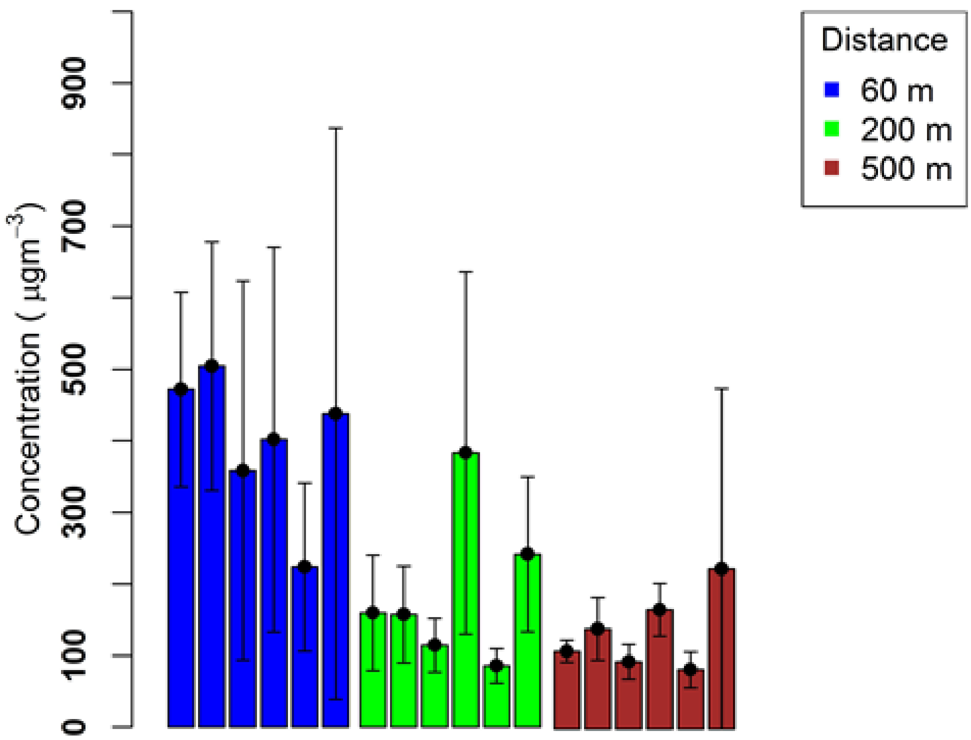

Figure 6a: Spatial variation of SO_2 concentration downwind of six gas flaring sites (adapted from Obanijesu et al. (2009))

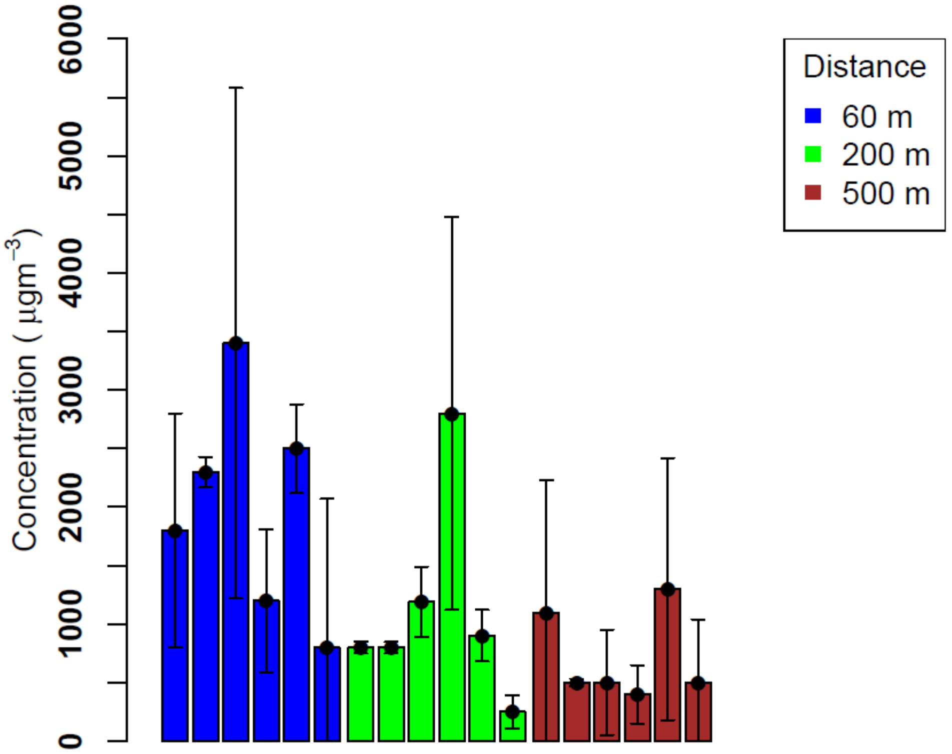

Figure 6b: Spatial variation of CO concentration downwind of six gas flaring sites (adapted from Sonibare et al. (2010))

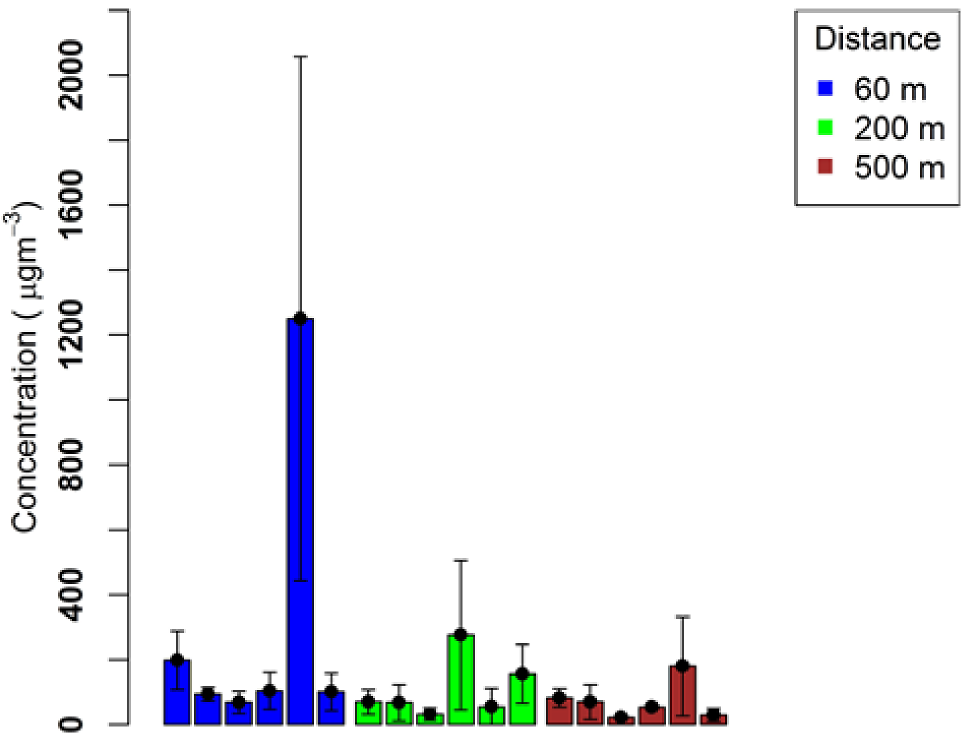

Figure 6c: Spatial variation of NO_2 concentration downwind of six gas flaring sites (adapted from Sonibare et al. (2010))

A summary of the few available in-situ ground measurements downwind of gas flaring sites in other regions of the world are given in Table 3.

Table 3: Pollutant measurements around several oil and gas facilities

BC ($ng\ kg^{-1}$)	**O_3 (ppbv)**	**VOC (ppbv)**	**PAH ($ng\ m^{-3}$)**	**NO (ppbv)**	**NO_2 (ppbv)**	**SO_2 (ppbv)**	**CO (ppbv)**	**Ref**
-	> 120	100 -350	-	> 3.5	> 7.5	-	> 80	Edwards et al. (2013)
> 40	> 25	-	-	> 1.2	-	> 1.2	> 90	(Roiger et al., 2015)
-	-	-	0.34 - 3.3×10^4	-	-	-	-	(Ana et al., 2012)

3.3 Types of Flares

Based on the design and operating condition of the system, flares can be categorised as *air-assisted*, *steam-assisted*, *non-assisted* and *pressure-assisted*. Flares are assisted primarily to enhance the turbulence and mixing of the fuel gas and air in the combustion zone, so as to suppress smoking of the resulting flame (Castineira and Edgar, 2006; Enviroware, 2012; Torres et al., 2012a). The choice of assistance, therefore, affects flame chemistry, as discussed below. Air and pressure-assisted flares are not as efficient as steam-assisted flares in terms of the carbon conversion efficiency (CCE) (Castineira and Edgar, 2006). Complete combustion of the fuel gas requires sufficient air for combustion and adequate mixing of the air and fuel gas. The efficiency of a gas flare at a given moment in time depends on the HHV of fuel gas (see table 2), design of the burner, mixing of air and fuel gas in the combustion zone, composition of the fuel gas, wind speed and direction, and ambient temperature and pressure (Kostiuk et al., 2004; Stone et al., 1992; Torres et al., 2012b).

Equivalence ratio, ϕ, is a measure of the amount of oxygen available for the combustion of the fuel gas (Flagan and Seinfeld, 2012; McAllister et al., 2011). It is defined as:

$$\phi = \frac{\left(\frac{A}{F}\right)_s}{\left(\frac{A}{F}\right)_a} \ldots\ldots\ldots\ldots\ldots\ldots\ldots\ldots\ldots\ldots\ldots\ldots \quad (2)$$

where $\left(\frac{A}{F}\right)_s$ is the stoichiometric air-fuel mass ratio and $\left(\frac{A}{F}\right)_a$ is the actual air-fuel mass ratio. $\phi < 1$ implies fuel-lean mixture, that is, more oxygen than is needed for the combustion of the fuel is available; $\phi = 1$, a stoichiometric mixture, where the exact amount of oxygen needed is made available, and $\phi > 1$, a fuel-rich mixture, less oxygen than is needed is available for the combustion of the fuel. Burners used in gas flaring and the entire gas flaring set-up are designed to produce a flame operating at $\phi \sim 1$ taking into account the economic aspects such as cost effectiveness of applying a process like steam assistance.

3.3.1 Steam- Assisted Flare

Steam-assisted flare involves the introduction of steam jet into the combustion zone of the flare to provide added momentum and turbulence to the fuel gas and air, enhancing mixing and as such suppressing the tendency for smoke in the flare (Castineira and Edgar, 2006; Müller-Dethlefs and Schlader, 1976; Stone et al., 1992). It is the most efficient assist given to flare to suppress smoking during combustion because the steam affects flame chemistry as well as mixing. The steam acts to break up long-chain hydrocarbons to smaller chains that burn with less smoke (Castineira and Edgar, 2006; Fortner et al., 2012; Müller-Dethlefs and Schlader, 1976; Torres et al., 2012a). Steam undergoes thermal dissociation in a flare flame to give H and OH free radicals that react with carbon to give CH_2- and –CHO radical moieties. The steam-induced free radicals enhance the formation of C=O bonds rather than C-C bonds, promoting completeness of combustion. The steam can also react with intermediate products like CO, oxidizing it further to CO_2 (Castineira and Edgar, 2006; Müller-Dethlefs and Schlader, 1976).

$$CO\,(g) + H_2O\,(g) \longrightarrow CO_2\,(g) + H_2\,(g) \qquad (\Delta H = -41\ \text{kJ mol}^{-1}) \quad \ldots\ldots\ldots \quad (3)$$

For a steam assisted flare, combustion efficiency starts to decrease when the steam-to-fuel gas ratio goes beyond a threshold which depends on the heat content of the fuel gas and the location at which the steam is injected into the combustion zone in the flare (USEPA, 2014).

In the US, a lower heating value (LHV) limit of 11.18 MJ/m^3 is imposed on fuel gas in order to be suitable for steam-assisted flares (Castineira and Edgar, 2006). Fuel gas with high heat content promotes higher combustion efficiency in steam-assisted flares (McDaniel and Tichenor, 1983; Torres et al., 2012b). Over-steaming results when too much steam is injected into the combustion zone; over-steaming is analogous to over-aeration in air-assisted flares. Over-steaming causes a decrease in the flame temperature by serving as a heat sink. A decrease in combustion efficiency of the flare results, along with, increased noise caused by cavitation created within the flame (Castineira and Edgar, 2006; Stone et al., 1992).

The formation of NO_X in steam-assisted flares is reduced, compared to non-assisted flares, and further reduced at large values of equivalence ratio (ϕ) due to a drop in the flame temperature (Miyauchi et al., 1981; Müller-Dethlefs and Schlader, 1976). Steam-assisted flares are rather expensive to maintain, especially for large gas facilities, as a large-scale steam generator is required.

3.3.2 Air-Assisted Flare

In air-assisted flares, forced air from a low-pressure blower is used as an additional source of momentum and turbulence to the fuel gas in the combustion zone and, hence, enhances the mixing of the fuel gas and air in the zone (Castineira and Edgar, 2006; Stone et al., 1992; Torres et al., 2012a). Air-assisted flaring involves the installation of an air blower that provides the forced air at the bottom of the stack. The major advantages of the air-assisted flare are that it is less expensive to run, extends the life-span of the flare by cooling the tip of the flare and is easier to maintain than other configurations (Castineira and Edgar, 2006). For an air-assisted flare, the combustion efficiency of the flare decreases linearly above a threshold limit of the air assist to fuel-gas ratio, but the rate of decrease is slow for a fuel gas with a higher VHV (Torres et al., 2012b). Incomplete combustion can occur when air-fuel gas ratios go beyond the optimum value, to the extent that the flame may be put out as a result of over-aeration (Castineira and Edgar, 2006).

3.3.3 Pressure-Assisted Flare

In pressure assisted flares, the fuel gas stream pressure is controlled by varying the volume flow of the fuel gas, and used to enhance the mixing of the fuel gas and air in the combustion zone. A high-pressure burner is used to promote atomization of any liquid hydrocarbon and enhance the mixing of the fuel gas with air to bring about a complete or near-complete combustion. Pressure assistance often requires significant amount of space in a remote area because of the burners arrangement at ground level. Fuel gas exit velocity increases with pressure at the burner. Pressure-assisted flares usually have burners arranged on the ground and as such must be located carefully within the oil and gas production plant (Enviroware, 2012; Stone et al., 1992).

3.3.4 Non-Assisted Flare

For non-assisted flares, no provision is given to provide momentum and enhanced mixing for the fuel gas and air. The method is often used for gases with low VHV, that is, fuel gas having low C-to-H ratio (in alkanes, C-to-H ratio increases from a minimum value of 0.25 for methane; see Table 2). The C-to-H ratio determines the smoking tendency of hydrocarbons, with smokiness increasing with C-to-H (USEPA, 1995). Note that the experimental fuel gas compositions listed in Table 2 are at or below the lowest C-to-H ratio of the Flow Station gas compositions listed. Non-assisted flaring is used for gases that require smaller amounts of air to undergo complete combustion (Enviroware, 2012; Stone et al., 1992).

Table 4 summarises the features of the different types of flares discussed in Section 3.3.

Table 4: Summary of the properties of flare types

	Steam-assisted	Air-assisted	Pressure-assisted	Non-assisted
Method	Steam is introduced into the combustion zone to enhance mixing.	Air is introduced from a blower to enhance the mixing and turbulence of the fuel gas in the combustion zone	The vent pressure of the gas flow is used to enhance mixing at the tip of the flare burner	No assistance is given to the combustion process
Efficiency	Most efficient in terms of suppressing soot formation. Some of the CO formed can be oxidized to CO_2	Less efficient than the steam assisted flare but relatively efficient that the other two types	Not as efficient as steam and air-assisted but can equally suppress sooting.	Only efficient for non-sooting combustion especially in light hydrocarbons
Benefits	Fuel with high heat value, and hence, high sooting propensity can be disposed of with relatively less soot	Prolongs the life span of the flare tip. Less expensive than steam-assisted and easy to maintain, hence, it is the most commonly used.	Enhance combustion efficiency when the gas flux pressure is sufficiently high enough without the additional cost of steam and air generation	Can be used for occasional emergency flaring of near smokeless gas
Relative size	They are often large flares as they include the steam generator and are usually employed in large gas facilities.	Not as large as the steam assisted.	May be of same size as air-assisted flare depending on the flow capacity of the facility	Often smaller in size compared to the other types
Shortcoming	Over-steaming can result in reduced efficiency of flare. It is also expensive to maintain on a large-scale	Over- aeration can also result in less efficiency. A limit of air assist to gas ratio must be maintained for effectiveness of the flare.	The fluctuation of gas flow pressure has a bearing consequence on the efficiency of the combustion. Requires large space in a remote area.	Cannot be used for dense fuels with high sooting propensity which are typical gas in oil and gas processing facilities

4 Estimating emissions from gas flaring

Emissions from a typical gas flare can be solids, liquids or gases. As a result of the inaccessible nature of full-scale real-world gas flares, several techniques have been used to quantify the amount of emissions from such flares. Such methods include measurement or source monitoring often by lab-based, pilot-study-based or field-based study (Johnson et al., 2011; McEwen and Johnson, 2012), application of emission factors obtained from measurements and scaling calculations (Giwa et al., 2014; Huang et al., 2015; Sonibare and Akeredolu, 2004; Talebi et al., 2014; USEPA, 1995) and, simulations, often by computational fluid dynamics (CFD) (Almanza et al., 2012).

In real-world flares, complete combustion cannot be achieved always and everywhere. Incomplete combustion of the fuel gas can be due to poor efficiency of the flare system, flame temperature (flame dynamical characteristics), insufficient oxygen resulting in poor stoichiometric air/fuel gas mixing ratio, the condition of the fuel gas in the combustion zone and prevailing ambient meteorological condition (Stone et al., 1992). Carbon monoxide (CO) can represent 24 – 80 % (on carbon a molar basis) of emissions for an incomplete combustion process (Torres et al., 2012b).

4.1 Determining the flame regime

It is important to define clearly the configuration of the fire (flare) as this is essential for an adequate estimation of the yield and transport of pollutant species from the combustion process. Flames can be classified along a spectrum ranging from turbulent diffusion flames (of the kinds discussed above) to pool fires (e.g. tar-pool fire) based on the nature and dynamics of the fuel in the flame as well as the design of the burning process (Delichatsios, 1987, 1993a). In this review we are concerned with gas flares, which are classified as turbulent jet-diffusion flames. They are so classified because of the high pressure associated with the release of the fuel gas into the flame.

Jet-diffusion flames in the environment can be categorized based on the momentum flux ratio, R, of the jet plume versus the horizontal momentum flux of the ambient wind (Huang and Wang, 1999). Flares with high R (R>10) may be further categorized depending on whether the flame characteristics are driven by the buoyancy of the hot plume or momentum of the fuel gas (McEwen and Johnson, 2012). Both buoyancy and momentum are important in determining the character of flares. A combination of several dimensionless parameters – Richardson number, Richardson ratio, fire Froude number, gas Froude number, and Reynolds number - have been used in studies to configure the regime of the flame in a jet-diffusion flame. The Froude numbers measure the ratio of the inertia force on an element of the fluid (in this case, gas or fire) to the weight of (i.e. gravitational force acting on) the fluid element. The fire Froude number, Fr_f, gas Froude number, Fr_g and Reynolds number, Re, have proved to be useful dimensionless parameter to define the flame regime (Becker and Liang, 1982; Delichatsios, 1993a; Delichatsios, 1993b; Delichatsios, 1987; Sivathanu and Faeth, 1990).

$$Fr_g = \frac{u_e {f_s}^{3/2}}{(g d_e)^{1/2} \left(\frac{\rho_e}{\rho_\infty}\right)^{1/4}} \quad \ldots\ldots (4)$$

$$Fr_f = \frac{u_e {f_s}^{3/2}}{\left(\frac{\Delta T_f}{T_\infty} g d_e\right)^{1/2} \left(\frac{\rho_e}{\rho_\infty}\right)^{1/4}} \quad \ldots\ldots (5)$$

$$Re_s = \frac{u_e d_e}{\upsilon_o} \quad \ldots\ldots (6)$$

$$f_s = \frac{1}{S+1} \quad \ldots\ldots (7)$$

In the definition of Fr_f in equation (5), $\left(\frac{\Delta T_f}{T_\infty}\right) g$ is the effective acceleration generated by individual hot eddies burning at the flame temperature (Delichatsios, 1987). Among the three dimensionless numbers defined by equations (4) - (6), the Reynolds number is used to determine the status of flow, either turbulent or laminar. The fire Froude number, Fr_f, is used to identify the dominant mechanism between buoyant-generated turbulence and momentum-generated turbulence. In practice, Fr_f can be used to parameterise soot yield from turbulent diffusion flames (Delichatsios, 1993b; McEwen and Johnson, 2012).

4.2 Emission factors (EF) for gas flaring emissions

The Emission factor (EF) of a pollutant is the amount of the pollutant released into the atmosphere per unit activity or per unit raw material consumed. It can be obtained from experimental measurements carried out on several sources which represent a particular emission source type. For example, road transport emission factor can be compiled by measuring the amount of each pollutant (CO_2, CO, PM, NO_x) given off by cars (petrol and diesel), heavy duty vehicles and motorbikes per litre of fuel burned for every km travelled (Gertler et al., 1998; USEPA, 1995; Zhang and Morawska, 2002) under given driving conditions. It is often expressed in g m^{-3} (pollutant produced per unit volume of raw material consumed), g kg^{-1} (pollutant produced per unit mass of raw material consumed), g km^{-1} (pollutant produced per unit distance travelled). Emission factors have been compiled by several agencies, which include the US Environmental Protection Agency (USEPA), the European Environmental Agency (EEA), the United Kingdom Department for Environment, Food and Rural Affairs (Defra), and GAINS (Greenhouse gas Air Pollution Interactions and Synergies), for several source categories based on technical sessions of lab-based studies, pilot studies or actual field measurements. Of these agencies, ECLIPSE and USEPA have EFs specifically for emissions from gas flares: the GAINS emission factor for BC from gas flaring is 1.6 g m^{-3}: the equivalent USEPA value has four discrete values between 0 and 6.4 g m^{-3} depending on the smokiness of the flame (see below). Stohl et al. (2013) in their study used emission factor of 1.6 g m^{-3} obtained from ECLIPSE (Evaluating the Climate and Air

Quality Impacts of Short-lived Pollutants) emissions data set to simulation BC emissions in the Arctic.

It is difficult to carry out an accurate estimate of emission from gas flares directly from field measurements. Conventional experimental techniques are not suited due to the severe operating conditions that occur in the flaring process and the almost uninhabitable nature of the gas flaring area to both man and the field equipment during the process of gas flaring (Ismail and Umukoro, 2014; McDaniel and Tichenor, 1983; McEwen and Johnson, 2012; RTI, 2011; Talebi et al., 2014). As a result of the unsteady and opaque nature of gas flare flames, remote sensing provides only a partial answer to the difficulties of in-situ monitoring.

In Chapter 13 of USEPA's 5th edition of the compilation of air pollutant emission factors known as AP-42, published in January 1995, emission factors (EF) for pollutant emitted from industrial flaring of waste gas were given; these were recently updated in 2014 (though still in the draft stage) except those for soot. The EFs published in 1995 were based on a study conducted by McDaniel and Tichenor (1983) aimed at determining combustion efficiency and hydrocarbon destruction efficiency for flares operated under different condition. The recent updates of EFs in AP-42 give emission factors of 0.17 kg GJ^{-1}, 1.43 kg GJ^{-1} and 0 - 6.4 g m^{-3} are given for CO, NOx and soot, respectively.

The fuel used in the pilot study to estimate EFs for industrial flare pollutants in the AP-42 compilation was predominantly propylene and inert diluents. As such, the EFs, especially for soot, might not be an adequate representation of a typical flare in the oil and gas industry with varying fuel gas composition (Table 2). For AP-42, the collection of soot at the experimental stage was not done by a conventionally accurate method. For instance, the particulate matter (soot) given off was not collected isokinetically in accordance with USEPA's method 5 for sampling particulate matter from stationary source (USEPA, 2000). An emission factor of 0.0

μg L^{-1} (microgram per litre of fuel gas at standard temperature and pressure) given for soot in non-smoking flares of industrial flares in AP-42 is of limited utility and presumably denotes a upper limit of 0.05 μg L^{-1}, because the soot yield from flares is never likely to be precisely zero. Even seemingly modest emission of soot (BC) can be significant, given what is now known of the effects of BC on climate, weather and human health from findings in recent studies (Bond et al., 2013; Ramanathan and Carmichael, 2008; Stocker et al., 2013; Tripathi et al., 2005; Wang et al., 2014).

The mass/mole balancing technique for estimating the yield of pollutants from the combustion of hydrocarbon is a widely used technique. Using this technique, Ismail and Umukoro (2014) and Sonibare and Akeredolu (2004) estimated the yield for SO_2, NO_X, CO_2 and CO from the combustion of fuel gas (hydrocarbon with inert diluents) at various levels of combustion. Both studies did not account for unburned carbon (soot) even for their 'severely' incomplete combustion process reactions. Ismail and Umukoro (2014) varied combustion efficiency (CE) and air available for combustion, and with CE as low as 0.5 (50 %) still did not account for unburned carbon.

4.3 Soot emission from gas flaring

Soot, which is predominantly black carbon (BC), is a product of the incomplete combustion of biomass, solid fuel and fossil fuel (Goldberg, 1985; Koch et al., 2009). Globally, fossil fuel combustion is estimated to contribute 3 Mt of BC to the atmosphere annually (Bond et al., 2004). Annually, the contribution of gas flaring to global BC concentration is estimated to be 260 Gg (Bond et al., 2013), that is approximately 0.1% of the total contribution from fossil-fuel use, of which Russia is estimated to contribute 81.0 Gg (Huang et al., 2015).

The formation and quantification of soot from the combustion of hydrocarbon is a rather complex thermo-chemical process that is not well understood, despite decades of research

(Castineira and Edgar, 2006; Haynes and Wagner, 1981; Johnson et al., 2011; Maricq, 2009). Soot given off from the combustion of hydrocarbon is predominantly elemental carbon and the amount given off depends on a number of factors, including the efficiency of the combustion process and the fire dynamical characteristics.

The diameter of soot particles emitted ranges between 10 – 200 nm and most commonly lies between 10 and 50 nm. Figure 7 shows a TEM micrograph of soot particle and agglomerates from acetylene flames. The very fine particle of soot are from seemingly 'non-sooting' flames while at the other extreme are those from heavily sooting flames (Flagan and Seinfeld, 2012; Glassman, 1996; Haynes and Wagner, 1981). Combustion of hydrocarbon components of the fuel gas has PAH and BC signatures which can be used as tracers for emissions from the flaring of fuel gas (Fortner et al., 2012; Maricq, 2009).

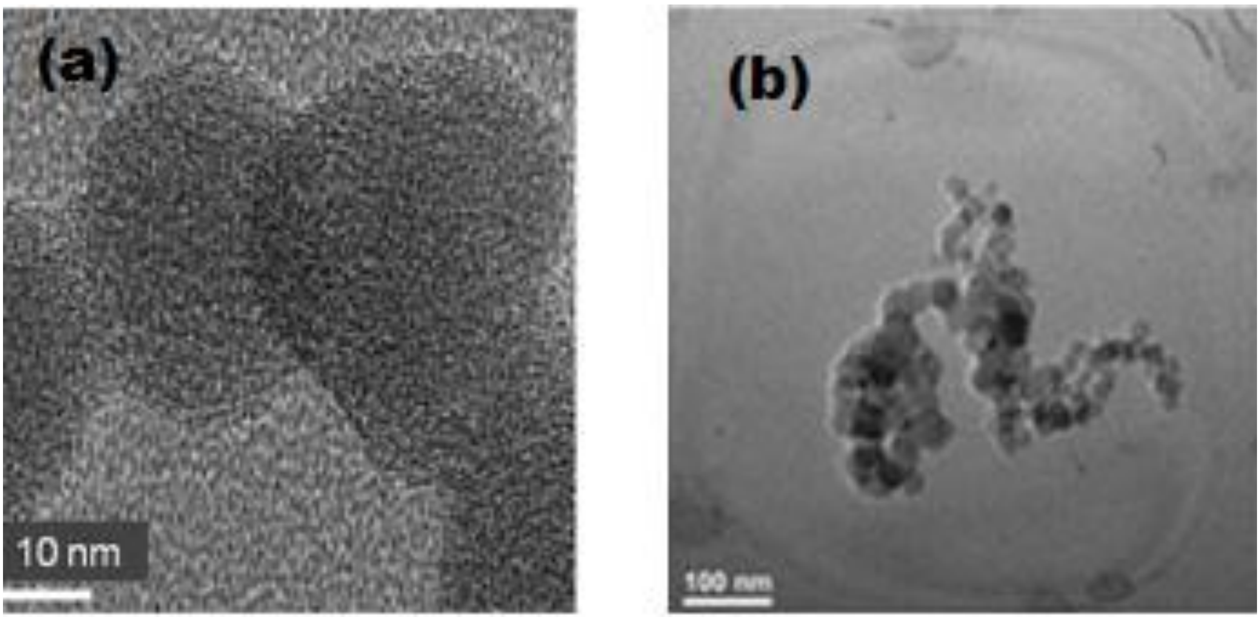

Figure 7: TEM micrograph of soot (a) microstructure (b) agglomerates (Tumolva et al., 2010).

Soot is formed when the carbon particles are cooled below their ignition temperature and there is a deficiency of oxygen (Stone et al., 1992). Considering the variation of the composition of gas flared from one station to the other, EFs available for estimating emissions from gas flares are overly generalised. The fuel gas used in most of the studies to estimate the EFs is either propylene or propane or a mixture of both with nitrogen added to alter the heat content as well as the use of predominantly methane-based fuels which are known to be low-sooting.

Several attempts have been made to quantify and study the characteristics of soot yield from gas flares using various approaches in lab-based, pilot-based and field-based studies as well as simulation techniques. Emission factors from some of these studies are given in Table 5. Other emission factors not highlighted in this table are based on the USEPA's AP-42 emission factors.

Table 5: A Summary of Emission Factors/Emission rate for Soot from Industrial Flares

Study (year)	Emission factor (g m^{-3} of fuel burned)	Emission rate (g s^{-1})	Type of study	Fuel
USEPA (1995)	0.0, 0.9, 4.2 6.4[a]	-	Pilot study	80% propylene 20% propane
Johnson et al. (2011)	-	2.0 (±0.66)	Field study	associated natural gas
Almanza et al. (2012)	-	0.025 – 0.22	CFD simulation	associated natural gas
McEwen and Johnson (2012)	0.51	-	Lab-scale flare	hydrocarbon (alkanes)
Johnson et al. (2013)	-	0.067	Field study	-
GAINS 2011	1.6	-	Modelling	-
IMP (2006)[b]	-	3.37	Simulation	associated natural gas
CAPP (2007)	2.563	-	-	associated natural gas

[a]0.0 is for *non-smoking* flame, 0.9 for *light smoking* flares, 4.2 for *averagely smoking* flare and 6.4 for *heavily smoking* flares

[b] cited in (Almanza et al., 2012)

The studies by Johnson et al. (2011) and Johnson et al. (2013) gave emission rates (g s^{-1}) and not emission factors (g m^{-3}) because both were actually field studies that quantified the soot given off per unit time by estimating the travel (speed) of the soot in space using a charge couple device camera (CCD) camera viewing a real field flare.

Emission of soot from the combustion of hydrocarbon varies with the VHV of the gas and, as such, the emission factor for soot can be estimated from its VHV (McDaniel and Tichenor, 1983; RTI, 2011; Torres et al., 2012b). McEwen and Johnson (2012), using a lab-based experiment, studied the BC emission from the combustion of hydrocarbon. The study varied the VHV of the fuel gas and measured the soot yield for each combustion process. The VHV used here is the higher heating value (HHV), or gross heating value. The relationship between the two variables (soot yield and HHV) obtained from the study by McEwen and Johnson (2012) is given in equation (8):

$$EF_{soot} = 0.0578(VHV) - 2.09 \qquad \text{……………………………….. (8)}$$

When the composition of the fuel gas is known, its VHV can be calculated from standard thermochemical tables (cf. Table 2). It should, however, be noted that because the VHV contains no information on flame dynamics, this relationship is only appropriate for the flame dynamics conditions of the experiment. Although, equation (8) is a readily available relationship to estimate soot emission from hydrocarbon combustion, its application is restricted to a complete or near-complete combustion process. Inserting the estimated VHV into the relation developed by McEwen and Johnson (2012) gives an estimate of the soot yield in g m^{-3}.

4.4 Scaling soot emission from lab-based studies

Lab-based studies of emissions from flares are the most common and readily available method to estimate emissions from full-scale flares. However, considering the size (diameter) of the flare stack, flow rate of fuel gas, exit velocity, and the resultant buoyancy of full-scale flare, there is a need to scale up the emissions yield from lab-based studies to be representative of a full scale flare. In earlier studies, several dimensionless parameter have been considered for such scaling purpose; these include Richardson ratio, Ri_L (Becker and Liang, 1982), fire Froude number, Fr_f (McEwen and Johnson, 2012), and the first Damköhler ratio, *Da₁* (Becker and Liang, 1982). Richardson ratio, Ri_L, is defined as the ratio of the buoyancy-generated turbulent kinetic energy (TKE) of the flame to the TKE of emitted gas jet at the exit:

$$Ri_L = \frac{gL^3}{(u_e d_e)^2}\left(\frac{\rho_\infty}{\rho_e}\right) \quad \text{...} (9)$$

Richardson ratio is the basis to assess the turbulent regime of the flame: when $Ri_L \ll 1$, buoyancy-induced mixing between emitted gas jet and background air is much weaker than jet-induced mixing, and consequently the flame is dominated by forced convection; when $Ri_L \gg 1$, jet-induced mixing is much weaker than buoyancy-induced mixing and the flame is dominated by natural convection. Fire Froude number, Fr_f, is defined in Equation (5) and can be interpreted as the ratio of the jet's inertia to the buoyancy force acting on it. Fire Froude number can be used to assess the dominating force to "stretch" the flame: when $Fr_f \gg 1$, the jet's momentum is the dominating factor and when $Fr_f \ll 1$, the flame's buoyancy force is the dominating factor. Comparing Fr_f against Ri_L, we understand that both are used to assess the dominating factor between jet-related quantity and buoyancy-related quantity, but there are two differences: (1) the quantity is momentum ($\propto$ velocity) for Fr_f, but TKE ($\propto$ velocity $\times$ velocity) for Ri_L; (2) the ratios between jet-related quantity and buoyancy-related quantity are reciprocal: $Ri_L \propto$ (buoyancy-related quantity)/(jet-related quantity) whereas $Fr_f \propto$ (jet-related quantity)/(buoyancy -related quantity). Therefore, these two parameters are closely related and mathematically their relationship should be $Ri_L \propto {Fr_f}^{-2}$. Precise relationship between them can be derived from Equations (5) and (9):

$$Ri_L = \left(\frac{\rho_\infty}{\rho_e}\right)^{3/2}\left(\frac{L}{d_e}\right)^3\left(\frac{T_\infty}{\Delta T_f}\right).{f_s}^3.{Fr_f}^{-2} \quad \text{..} (10)$$

It is noted that $\left(\frac{L}{d_e}\right)^3$ can be interpreted as the volume expansion ratio of the flaring gas due to burning and $\left(\frac{T_\infty}{\Delta T_f}\right)^{-1}$ can be approximated as the temperature rising ratio of the flaring gas due to burning. Based on the gas law, these two are proportional to each other for an isobaric process (from the exit to the flame tip) which is a good assumption for gas flaring, i.e. $\left(\frac{L}{d_e}\right)^3 \propto \left(\frac{T_\infty}{\Delta T_f}\right)^{-1}$, or equivalently, $\left(\frac{L}{d_e}\right)^3 \left(\frac{T_\infty}{\Delta T_f}\right) \approx \text{const}$. Therefore, Equation (10) confirms the relationship of $Ri_L \propto {Fr_f}^{-2}$. This suggests a strong dependence between adopting Ri_L and adopting Fr_f as the scaling parameter.

The first Damköhler ratio, *Da₁*, however, is defined as the ratio of residence time of fuel in flame (τ_{res}) to chemical time of burning process (τ_{chem}):

$$Da_1 = \frac{residence\ time\ in\ flame, \tau_{res}}{chemical\ time,\ \tau_{chem}} = \left(\frac{L}{u_e}\right) \Big/ \tau_{chem} \quad \ldots\ldots\ldots\ldots\ldots\ldots\ldots\ldots\ldots (11)$$

It describes the extent of the oxidation process within the flame in relation to the oxidant's feed rate. For a large Da_1 (i.e. $\tau_{res} \gg \tau_{chem}$), the velocity fluctuating component does not have much influence on the chemistry of the flame. The chemical reaction is able to proceed to completion within the residence time in the combustion zone, resulting in intensive chemical reaction and hot diffusion flame. For a small Da_1 (i.e. $\tau_{chem} \gg \tau_{res}$), turbulence can significantly affect the chemistry and structure of the flame. The rate of chemical reaction and hence, heat release may be affected, causing combustion product to be mixed with reactants within a time interval shorter than the chemical reaction time (Liberman, 2010; William, 1985). From the perspective of processes, Da_1 involves an extra dimension (i.e. chemical processes) which is not reflected by either Ri_L or Fr_f. In principle, we should consider Da_1 as one more scaling parameter.

4.5 Soot modelling

Mathematical modelling is a technique that has been used by scientist and engineers over the years to understand the relationship between sets of input and output parameters in a process, especially where the 'real world' process is often remote or grossly complicated to assess. The region of validity of such model outputs is often limited as several assumptions and constants are applied in the modelling to further simplify the process being studied.

Soot formation and oxidation in pre-mixed and non-premixed (diffusion) hydrocarbon flames have been studied using several modelling techniques including computational fluid dynamics (CFD). The main problem with mathematical modelling of turbulent combustion of hydrocarbon is the problem of modelling turbulent flow and chemical kinetics and the interaction between flow and chemical reaction (Magnussen and Hjertager, 1977). Kennedy (1997) classified the models for soot formation as empirical correlations, semi-empirical correlation models and models with detailed chemistry and physics of soot formation. The flame temperature, C:H ratio and number of carbon atoms in the fuel (hydrocarbon) are important parameters considered to have strong influence on the sooting propensity of the hydrocarbon (Harris et al., 1986). These parameters have been the basis of measurements used in most empirical correlation models.

In their study to modelling soot formation and combustion, Magnussen and Hjertager (1977) assumed that soot is formed from a gaseous hydrocarbon in two stages (a) formation of radical nuclei, and (b) soot particle formation from these nuclei. Applying expressions for the rate of formation of radical nuclei and rate of soot particle formation expressions developed by Tesner et al. (1971a); (Tesner et al., 1971b) in their model, tested on both pre-mixed and diffusion flame, they predicted soot concentrations that are in close agreement with experimental data. They concluded that soot formed and was contained in eddies and burned away during turbulence dissipation.

Moss et al. (1989), using a two-equation model for the evolution of soot volume fraction and number density, simulated the formation of soot. They included the influences of nucleation, surface growth and coagulation on the rate of soot formation. As given in equations 12(a) and (b), their model contains simplified expressions to quantify particle nucleation, growth and coagulation; using three empirical constants that are dependent on the fuel to control the rate of these processes. A major finding from their study is that soot volume fraction is proportional to the square of pressure.

$$\left\{\frac{d(\frac{n}{N_o})}{dt}\right\} = \alpha(\zeta) - \beta(\zeta)(\frac{n}{N_0})^2 \quad \text{.......... 12(a)}$$

$$\rho_s \left\{\frac{df_v}{dt}\right\} = \gamma(\zeta)n + \delta(\zeta) \quad \text{.......... 12(b)}$$

where ρ_s is the assumed density for solid carbon (1.8 x 10^3 kgm^{-3}), N_o is Avogadro's number and ζ is the mixture fraction. Rates of the processes are expected to be a function of the mixture fraction. The rates of the processes are defined explicitly in terms of the fuel density, ρ, temperature. T, and fuel mole fraction, X_c as described in equation 13:

$$\left.\begin{aligned} &\alpha \equiv C_\alpha \rho^2 T^{1/2} X_c \exp\left({}^{-T_\alpha}/_{T}\right);\ \beta \equiv C_\beta T^{1/2} \\ &\gamma \equiv C_\gamma \rho T^{1/2} X_c \exp\left({}^{-T_\gamma}/_{T}\right);\ \delta \equiv C_\delta \alpha \end{aligned}\right\} \quad \text{.......... 13}$$

coefficients $C_{\alpha,\beta,\gamma,\delta}$ and activation temperatures, T_α and T_γ are obtained from experimental data. In equations 12(a), the first and second term on the left are nucleation and coagulation processes, respectively. And, in equation 12(b), the first and second term on the left represent the growth and nucleation, respectively.

Lautenberger et al. (2005) developed a CFD model to study the formation and oxidation of soot. Since their model was to generate enough accurate predictions of soot emission concentrations in order to estimate CFD simulations of fire radiation from turbulent flames, considerations were given only to phenomena which were essential. Soot estimation in their model was based on a further simplified form of the two-equation model of Moss et al. (1989). There are no fuel-specific constants in their estimations, but rather, they used the laminar smoke point height to account for the sooting propensity of different fuels. The smoke point of a flame is its length just before the onset of the release of visible smoke. Length of a flame is dependent on the extent of completeness of the combustion and heat content of the fuel gas (Beychok, 1994).

The use of CFD simulation soot has made it possible to make predictions about the relationships between the various processes involved in soot formation and oxidation in both pre-mixed and diffusion hydrocarbon flames as well as the sensitivity of the soot formation to some of the complex phenomena. However, the veracity of CFD simulation results in limited by the availability of field measurements for model evaluation.

4.6 Gas flaring emissions in global models and inventories

To the best of our knowledge, the only two emission datasets that explicitly includes gas flaring emissions are EDGAR (Emissions Database for Global Atmospheric Research) and ECLIPSE (Evaluating the Climate and Air Quality ImPacts of Short-livEd Pollutants) gridded emissions datasets.

In EDGAR v4.2, for gas venting and flaring, emissions were calculated for 1994 onwards using the amount of gas flared estimated from satellite observations of intensities of light from various gas flares. The estimated quantities of gas flared and emission factors obtained from either inventory guidance documents or confidential information were used to generate gridded annual emission datasets for different countries on a resolution of 0.1^o x 0.1^o. In 2005, the inclusion of new primary data sources for gas flaring in EDGAR v4.2 gives rise to a change of +75 % of EDGAR 4.1 value (130 Tg) in global CO_2 emission (European Commission, 2009).

ECLIPSE is provided by the IIASA (International Institute for Applied Systems Analysis). Emission calculations for the historical years (2005 – 2010) were developed in a series of regional and global projects. For gas flaring, emissions were calculated using data available from NOAA, NASA and the World Bank collaborative work to estimate the volume of gas flared globally. The volume of gas flared was estimated using NASA MODIS active fire detection products (Elvidge et al., 2007; Elvidge et al., 2011). Emission factors and other parameterizations were obtained from peer-reviewed data on emission performance of various technologies. The calculation was performed with the IIASA GAINS model (Klimont et al., 2013). The ECLIPSE v4 global emission dataset is available on a 0.5^o x 0.5^o lon-lat resolution.

Stohl et al. (2013), performing a 3-year black carbon (BC) simulation in the Arctic, using a Lagrangian particle dispersion model FLEXPART driven by the ECLIPSE dataset, estimated that more than 40 % of mean surface BC surface concentration in the Arctic is attributable to gas flaring. Although, more studies on the sensitivity of global models to gas flaring emission is needed to give a clear and precise quantification of the contribution of gas flaring emission to global aerosol loadings, the change in global CO_2 level in EDGAR4.2 underscores the importance of an explicit inclusion of gas flaring emissions in global models.

5 Conclusion

The World Bank has been at the fore-front of the campaign to reduce gas flaring through the public-private partnership project “Global Gas Flaring Reduction (GGFR)” (http://www.worldbank.org/en/programs/gasflaringreduction). The "Zero Routine Flaring by 2030" initiative was launched in April 2015 by the World Bank, United Nations, governments and oil companies. As at April 17 2015, a total of nine countries have agreed to the "Zero Routine Flaring by 2030" initiative. At the time of writing, some major flaring nations have yet to sign up to the initiative. Indeed, some major flaring countries still struggle to meet targets for gas flaring set in the late 1980s. A steep increase in flaring since 2006 has been reported for the USA and Canada, associated, presumably, with the exploitation of unconventional hydrocarbon reservoirs.

Considering the wide spectrum, quantity and effects of pollutants emitted from gas flaring, coupled with the estimated quantity of gas flared globally, it is surprising that so little effort has been put into adequately understanding the yield of pollutants, especially BC, from the process in real world field situations. The wide variation of fuel gas compositions from flow stations around the world underpins the importance of developing strategies that take these compositions into consideration when estimating emissions.

The steep decrease in the fraction of total gas production flared between 2000 and 2006 seems to have stabilised between 2007 and 2010, and the fraction has even increased in 2011. The overall quantity of gas flared since 2000 has been steady between 93 and 110 bcm. An increase in total production since 2009 has brought about a corresponding increase in the quantity of gas flared. Incentives and stringent policies are not yet in place to encourage more companies and countries to partner with the World Bank in their "Zero Routine Flaring by 2030" initiative.

Elevated concentrations of BC, CO, H_2S, SO_2, NO, NO_2 and PAH measured around flaring sites (ground based and aircraft) is indicative of the detrimental impact of gas flaring on the environment. Clusters of gas flaring sites around the tropics and near-tropic regions of the world, where there is the likelihood on enhanced atmospheric mixing of the emissions into the lower and even mid-troposphere, coupled with the high temperature of the emitted plume suggests the possibility of long-range transport of these pollutants.

Emission factors used for BC emission from gas flaring are inadequate to estimate emission from a typical real-world gas flare as most of the fuels used in the studies for such emission factors are not representative of fuel gas from most Flow Stations around the world. In the studies that employed the mass/mole balancing technique to estimate pollutants from the combustion of hydrocarbons, estimated EFs for CO_2 and CO have been given, but there is no consideration of the amount of unburnt carbon given off. It should be noted that these studies did not consider flame dynamics changes in their estimations. When estimating emissions from gas flares, there is the need to ascertain the nature (regime) of the combustion flame as the flame nature and temperature plays pivotal role in determining the pollutants yield, and this has not yet been routinely considered in dispersion modelling and global inventories.

Global models need to update the sources of BC to include gas flaring, especially in regions prone to long-range transfer of gas flaring emission from leading gas flaring nations including Russia, Nigeria and the Middle East.

Acknowledgment

Olusegun G. Fawole is highly grateful to the UK government for funding his PhD studies through the UK Commonwealth Scholarships Commission (CSCUK). The authors appreciates the anonymous reviewers for their helpful criticisms and comments.

6 Glossary

1. Heating value – the heat evolved per unit of a gas when it undergoes complete combustion at standard temperature and pressure. It can be measured in unit mass, unit mole or unit volume.
2. Higher (gross) heating value (HHV) – The heating value when all of the water present in the combustion product in gas phase condenses to liquid.
3. Lower (net) heating value (LHV) - The heating value when all of the water present in the combustion product remains in the gas phase.
4. Volumetric heating value (VHV) – Total heat evolved per unit volume of a gas.
5. Equivalent ratio, ϕ - This is the ratio of the stoichiometric air-fuel mass ratio to the actual air-fuel mass ratio
6. Mtoe – Million tonnes of oil equivalent
7. Laminar smoke point - The length of flame from a gas jet just before the onset of the release of visible smoke.

7 References

Abdulkareem, A. and Odigure, J., 2006. Deterministic Model for Noise Dispersion from gas Flaring: A case study of Niger–Delta area of Nigeria. Chemical and biochemical engineering quarterly, 20(2): 157-164.

Almanza, V., Molina, L. and Sosa, G., 2012. Soot and SO 2 contribution to the supersites in the MILAGRO campaign from elevated flares in the Tula Refinery. Atmospheric Chemistry and Physics, 12(21): 10583-10599.

Ana, G., Sridhar, M. and Emerole, G., 2012. Polycyclic aromatic hydrocarbon burden in ambient air in selected Niger Delta communities in Nigeria. Journal of the Air & Waste Management Association, 62(1): 18-25.

Arctic Council, 2013. Recommendations to reduce black carbon and methane emissions to slow Arctic climate change, Arctic task force on short-lived climate forcers.

Avwiri, G. and Nte, F., 2004. Environmental sound quality of some selected flow stations in the Niger Delta of Nigeria. Journal of Applied Sciences and Environmental Management, 7(2): 75-77.

Barry, R.G. and Chorley, R.J., 2009. Atmosphere, weather and climate. Routledge.

Becker, H. and Liang, D., 1982. Total emission of soot and thermal radiation by free turbulent diffusion flames. Combustion and Flame, 44(1): 305-318.

Beychok, M.R., 1994. Fundamentals of stack gas dispersion, 63. Milton R. Beychok Irvine.

Bond, T.C., Doherty, S.J., Fahey, D., Forster, P., Berntsen, T., DeAngelo, B., Flanner, M., Ghan, S., Kärcher, B. and Koch, D., 2013. Bounding the role of black carbon in the climate system: A scientific assessment. Journal of Geophysical Research: Atmospheres, 118(11): 5380-5552.

Bond, T.C., Streets, D.G., Yarber, K.F., Nelson, S.M., Woo, J.H. and Klimont, Z., 2004. A technology-based global inventory of black and organic carbon emissions from combustion. Journal of Geophysical Research: Atmospheres (1984–2012), 109(D14).

BP, 2013. Statistical review of world energy, British Petroleum, Great Britain www.bp.com/statisticalreview.

BP, 2015. BP Statistical Review of world energy (www.bp.com/statisticalreview).

Burney, J. and Ramanathan, V., 2014. Recent climate and air pollution impacts on Indian agriculture. Proceedings of the National Academy of Sciences: 201317275.

CAPP, 2007. A recommended approach to completing the national pollutant release inventory (NPRI) for the upstream oil and gas industry, Canadian Association of Petroleum Producers, Calgary, Canada.

Casadio, S., Arino, O. and Serpe, D., 2012. Gas flaring monitoring from space using the ATSR instrument series. Remote Sensing of Environment, 116: 239-249.

Castineira, D. and Edgar, T.F., 2006. CFD for simulation of steam-assisted and air-assisted flare combustion systems. Energy & fuels, 20(3): 1044-1056.

Chung, S.H. and Seinfeld, J.H., 2005. Climate response of direct radiative forcing of anthropogenic black carbon. Journal of Geophysical Research: Atmospheres (1984–2012), 110(D11).

Davoudi, M., Rahimpour, M., Jokar, S., Nikbakht, F. and Abbasfard, H., 2013. The major sources of gas flaring and air contamination in the natural gas processing plants: a case study. Journal of Natural Gas Science and Engineering, 13: 7-19.

Delichatsios, M., 1993a. Smoke yields from turbulent buoyant jet flames. Fire safety journal, 20(4): 299-311.

Delichatsios, M., 1993b. Transition from momentum to buoyancy-controlled turbulent jet diffusion flames and flame height relationships. Combustion and flame, 92(4): 349-364.

Delichatsios, M.A., 1987. Air entrainment into buoyant jet flames and pool fires. Combustion and Flame, 70(1): 33-46.

Dung, E.J., Bombom, L.S. and Agusomu, T.D., 2008. The effects of gas flaring on crops in the Niger Delta, Nigeria. GeoJournal, 73(4): 297-305.

E & P Forum, 1994. Methods of estimating atmospheric emission from E&P operations; OGP Report No. 2.59/197 The Oil Industry International Exploration and Production forum, 25-28 Old Burlington street, London. http://www.ogp.org.uk/pubs/197.pdf

Edwards, P., Young, C., Aikin, K., deGouw, J., Dubé, W., Geiger, F., Gilman, J., Helmig, D., Holloway, J. and Kercher, J., 2013. Ozone photochemistry in an oil and natural gas extraction region during winter: simulations of a snow-free season in the Uintah Basin, Utah. Atmospheric Chemistry and Physics, 13(17): 8955-8971.

Edwards, P.M., Brown, S.S., Roberts, J.M., Ahmadov, R., Banta, R.M., deGouw, J.A., Dube, W.P., Field, R.A., Flynn, J.H., Gilman, J.B., Graus, M., Helmig, D., Koss, A., Langford, A.O., Lefer, B.L., Lerner, B.M., Li, R., Li, S.-M., McKeen, S.A., Murphy, S.M., Parrish, D.D., Senff, C.J., Soltis, J., Stutz, J., Sweeney, C., Thompson, C.R., Trainer, M.K., Tsai, C., Veres, P.R., Washenfelder, R.A., Warneke, C., Wild, R.J., Young, C.J., Yuan, B. and Zamora, R., 2014. High winter ozone pollution from carbonyl photolysis in an oil and gas basin. Nature, advance online publication.

Elvidge, C.D., Baugh, K., Pack, D., Milesi, C. and Erwin, E., 2007. A twelve year record of national and global gas flaring volumes estimated using satellite data. Boulder, CO, NOAA National Geophysical Data Center.

Elvidge, C.D., Baugh, K.E., Ziskin, D., Anderson, S. and Ghosh, T., 2011. Estimation of gas flaring volumes using NASA MODIS fire detection products. NOAA National Geophysical Data Center (NGDC), annual report, 8.

Elvidge, C.D., Zhizhin, M., Baugh, K., Hsu, F.-C. and Ghosh, T., 2015. Methods for Global Survey of Natural Gas Flaring from Visible Infrared Imaging Radiometer Suite Data. Energies, 9(1): 14.

Elvidge, C.D., Ziskin, D., Baugh, K.E., Tuttle, B.T., Ghosh, T., Pack, D.W., Erwin, E.H. and Zhizhin, M., 2009. A fifteen year record of global natural gas flaring derived from satellite data. Energies, 2(3): 595-622.

Enviroware, 2012. Modelling industrial flares impacts, http://www.enviroware.com.

European Commission, 2009. Emission Database for Global Atmospheric Research (EDGAR), release version 4.0. http://edgar.jrc.ec.europa.eu, Joint Research Centre (JRC)/Netherlands Environmental Assessment Agency (PBL), Netherlands.

Feichter, J. and Stier, P., 2012. Assessment of black carbon radiative effects in climate models. Wiley Interdisciplinary Reviews: Climate Change, 3(4): 359-370.

Flagan, R.C. and Seinfeld, J.H., 2012. Fundamentals of air pollution engineering. Courier Dover Publications.

Flanner, M.G., Zender, C.S., Randerson, J.T. and Rasch, P.J., 2007. Present-day climate forcing and response from black carbon in snow. Journal of Geophysical Research: Atmospheres (1984–2012), 112(D11).

Fortner, E., Brooks, W., Onasch, T., Canagaratna, M., Massoli, P., Jayne, J., Franklin, J., Knighton, W., Wormhoudt, J. and Worsnop, D., 2012. Particulate Emissions Measured During the TCEQ Comprehensive Flare Emission Study. Industrial & Engineering Chemistry Research, 51(39): 12586-12592.

Gertler, A.W., Sagebiel, J.C., Dippel, W.A. and Farina, R.J., 1998. Measurements of dioxin and furan emission factors from heavy-duty diesel vehicles. Journal of the Air & Waste Management Association, 48(3): 276-278.

GGFR, 2012. Estimated Flared Volumes from Satellite Data, 2007-2011., Global Gas Flaring Reduction, http://go.worldbank.org/G2OAW2DKZ0 (last accessed on January 9, 2015).

GGFR, 2013. The news flare (issue 14), Washington DC ; World Bank. http://documents.worldbank.org/curated/en/2013/06/18082251/news-flare-issue-14.

Giwa, S.O., Adama, O.O. and Akinyemi, O.O., 2014. Baseline black carbon emissions for gas flaring in the Niger Delta region of Nigeria. Journal of Natural Gas Science and Engineering, 20: 373-379.

Glassman, I., 1996. Combustion. Academic Press

Goldberg, E.D., 1985. Black carbon in the environment: properties and distribution. Environmental science and technology (USA).

Harris, M.M., King, G.B. and Laurendeau, N.M., 1986. Influence of temperature and hydroxyl concentration on incipient soot formation in premixed flames. Combustion and flame, 64(1): 99-112.

Haynes, B. and Wagner, H.G., 1981. Soot formation. Progress in Energy and Combustion Science, 7(4): 229-273.

Hodgson, S., Nieuwenhuijsen, M.J., Colvile, R. and Jarup, L., 2007. Assessment of exposure to mercury from industrial emissions: comparing "distance as a proxy" and dispersion modelling approaches. Occupational and environmental medicine, 64(6): 380-388.

Holden, J., 2005. An introduction to physical geography and the environment. Pearson Education.

Huang, K., Fu, J.S., Prikhodko, V.Y., Storey, J.M., Romanov, A., Hodson, E.L., Cresko, J., Morozova, I., Ignatieva, Y. and Cabaniss, J., 2015. Russian anthropogenic black carbon: Emission reconstruction and Arctic black carbon simulation. Journal of Geophysical Research: Atmospheres.

Huang, R.F. and Wang, S.M., 1999. Characteristic flow modes of wake-stabilized jet flames in a transverse air stream. Combustion and Flame, 117(1): 59-77.

IEA, 2012. IEA statistics: Natural gas information, International Energy Agency.

IEA, 2013. Key World Energy Statistics International Energy Agency, France.

IMP, 2006. Estudio de las emisiones de la zona industrial de Tula y su impacto en la calidad del aire regional , PS-MA-IF-F21393-1, IMP, Mexico.

IPCC, 2007. Climate Change 2007: The Physical Science Basis. Contribution of Working Group I to the Fourth Assessment Report of the Intergovernmental Panel on Climate Change [Solomon, S., D. Qin, M. Manning, Z. Chen, M. Marquis, K.B. Averyt, M.Tignor and H.L. Miller (eds.)]. Cambridge University Press, Cambridge, United Kingdom and New York, NY, USA.

Ismail, O.S. and Umukoro, G.E., 2014. Modelling combustion reactions for gas flaring and its resulting emissions. Journal of King Saud University-Engineering Sciences: http:dx.doi.org/10.1016/j.jksues.2014.02.003.

Jacobson, M.Z., 2002. Control of fossil-fuel particulate black carbon and organic matter, possibly the most effective method of slowing global warming. Journal of Geophysical Research: Atmospheres (1984–2012), 107(D19): ACH 16-1-ACH 16-22.

Johansson, J.K., Mellqvist, J., Samuelsson, J., Offerle, B., Lefer, B., Rappenglück, B., Flynn, J. and Yarwood, G., 2014. Emission measurements of alkenes, alkanes, SO2, and NO2 from stationary sources in Southeast Texas over a 5 year period using SOF and mobile DOAS. Journal of Geophysical Research: Atmospheres, 119(4): 1973-1991.

Johnson, M., Devillers, R. and Thomson, K., 2013. A Generalized Sky-LOSA Method to Quantify Soot/Black Carbon Emission Rates in Atmospheric Plumes of Gas Flares. Aerosol Science and Technology, 47(9): 1017-1029.

Johnson, M.R. and Coderre, A.R., 2011. An analysis of flaring and venting activity in the Alberta upstream oil and gas industry. Journal of the Air & Waste management association, 61(2): 190-200.

Johnson, M.R., Devillers, R.W. and Thomson, K.A., 2011. Quantitative field measurement of soot emission from a large gas flare using Sky-LOSA. Environmental science & technology, 45(1): 345-350.

Kennedy, I.M., 1997. Models of soot formation and oxidation. Progress in Energy and Combustion Science, 23(2): 95-132.

Klimont, Z., Smith, S.J. and Cofala, J., 2013. The last decade of global anthropogenic sulfur dioxide: 2000–2011 emissions. Environmental Research Letters, 8(1): 014003.

Koch, D., Schulz, M., Kinne, S., McNaughton, C., Spackman, J.R., Balkanski, Y., Bauer, S., Berntsen, T., Bond, T.C. and Boucher, O., 2009. Evaluation of black carbon estimations in global aerosol models. Atmospheric Chemistry and Physics, 9(22): 9001-9026.

Kostiuk, L., Johnson, M. and Thomas, G., 2004. University Of Alberta Flare Research Project: final report November 1996-September 2004. 2, http://www.mece.ualberta.ca/groups/combustion/flare/papers/Final%20Report2004.pdf.

Lautenberger, C.W., de Ris, J.L., Dembsey, N.A., Barnett, J.R. and Baum, H.R., 2005. A simplified model for soot formation and oxidation in CFD simulation of non-premixed hydrocarbon flames. Fire Safety Journal, 40(2): 141-176.

Law, K., Fierli, F., Cairo, F., Schlager, H., Borrmann, S., Streibel, M., Real, E., Kunkel, D., Schiller, C. and Ravegnani, F., 2010. “Air mass origins influencing TTL chemical composition over West Africa during 2006 summer monsoon” published in Atmos. Chem. Phys., 10, 10753–10770, 2010. Atmos. Chem. Phys, 10: 10939-10940.

Leahey, D. and Davies, M., 1984. Observations of plume rise from sour gas flares. Atmospheric Environment (1967), 18(5): 917-922.

Leahey, D.M., Preston, K. and Strosher, M., 2001. Theoretical and observational assessments of flare efficiencies. Journal of the Air & Waste Management Association, 51(12): 1610-1616.

Liberman, M.A., 2010. Introduction to physics and chemistry of combustion: explosion, flame, detonation. Springer Science & Business Media.

MacKay, D., 2008. Sustainable Energy-without the hot air. UIT Cambridge.

Magnussen, B.F. and Hjertager, B.H., 1977. On mathematical modeling of turbulent combustion with special emphasis on soot formation and combustion, Symposium (International) on Combustion. Elsevier, pp. 719-729.

Mari, C.H., Reeves, C.E., Law, K.S., Ancellet, G., Andrés-Hernández, M.D., Barret, B., Bechara, J., Borbon, A., Bouarar, I. and Cairo, F., 2011. Atmospheric composition of West Africa: highlights from the AMMA international program. Atmospheric Science Letters, 12(1): 13-18.

Maricq, M.M., 2009. An examination of soot composition in premixed hydrocarbon flames via laser ablation particle mass spectrometry. Journal of Aerosol Science, 40(10): 844-857.

Mathon, V. and Laurent, H., 2001. Life cycle of Sahelian mesoscale convective cloud systems. Quarterly Journal of the Royal Meteorological Society, 127(572): 377-406.

McAllister, S., Chen, J.-Y., Fernandez-Pello, A.C., Fernandez-Pello, A.C. and Fernandez-Pello, A.C., 2011. Fundamentals of combustion processes. Springer.

McDaniel, M. and Tichenor, B.A., 1983. Flare efficiency study, US Environmental Protection Agency, Industrial Environmental Research Laboratory, http://www.tceq.state.tx.us/assets/public/implementation/air/rules/Flare/Resource_1.pdf.

McEwen, J.D. and Johnson, M.R., 2012. Black carbon particulate matter emission factors for buoyancy-driven associated gas flares. Journal of the Air & Waste Management Association, 62(3): 307-321.

Miyauchi, T., Mori, Y. and Yamaguchi, T., 1981. Effect of steam addition on NO formation, Symposium (International) on combustion. Elsevier, pp. 43-51.

Moss, J., Stewart, C. and Syed, K., 1989. Flowfield modelling of soot formation at elevated pressure, Symposium (International) on Combustion. Elsevier, pp. 413-423.

Müller-Dethlefs, K. and Schlader, A., 1976. The effect of steam on flame temperature, burning velocity and carbon formation in hydrocarbon flames. Combustion and flame, 27: 205-215.

Nwaichi, E.O. and Uzazobona, M.A., 2011. Estimation of the CO2 Level due to Gas Flaring in the Niger Delta. Research Journal of Environmental Sciences, 5(6): 565-572.

Obanijesu, E., Adebiyi, F., Sonibare, J. and Okelana, O., 2009. Air-borne SO2 Pollution Monitoring in the Upstream Petroleum Operation Areas of Niger-Delta, Nigeria. Energy Sources, Part A, 31(3): 223-231.

OGP, 2000. Flaring and venting in the oil and gas exploration and production industry: An overview of purpose, quantities, issues, practices and trends. Report No. 2.79/288, International association of oil and gas producers UK http://www.ogp.org.uk/pubs/288.pdf.

Osuji, L.C. and Adesiyan, S.O., 2005. The Isiokpo Oil-Pipeline Leakage: Total Organic Carbon/Organic Matter Contents of Affected Soils. Chemistry & biodiversity, 2(8): 1079-1085.

Osuji, L.C. and Onojake, C.M., 2004. Trace Heavy Metals Associated with Crude Oil: A Case Study of Ebocha-8 Oil-Spill-Polluted Site in Niger Delta, Nigeria. Chemistry & biodiversity, 1(11): 1708-1715.

Ouf, F.-X., Vendel, J., Coppalle, A., Weill, M. and Yon, J., 2008. Characterization of soot particles in the plumes of over-ventilated diffusion flames. Combustion Science and Technology, 180(4): 674-698.

Pope III, C.A., Burnett, R.T., Thun, M.J., Calle, E.E., Krewski, D., Ito, K. and Thurston, G.D., 2002. Lung cancer, cardiopulmonary mortality, and long-term exposure to fine particulate air pollution. Journal of American Medical Association, 287(9): 1132-1141.

Quinn, P., Bates, T., Baum, E., Doubleday, N., Fiore, A., Flanner, M., Fridlind, A., Garrett, T., Koch, D. and Menon, S., 2008. Short-lived pollutants in the Arctic: their climate impact and possible mitigation strategies. Atmospheric Chemistry and Physics, 8(6): 1723-1735.

Ramana, M., Ramanathan, V., Feng, Y., Yoon, S., Kim, S., Carmichael, G. and Schauer, J., 2010. Warming influenced by the ratio of black carbon to sulphate and the black-carbon source. Nature Geoscience, 3(8): 542-545.

Ramanathan, V. and Carmichael, G., 2008. Global and regional climate changes due to black carbon. Nature geoscience, 1(4): 221-227.

Reeves, C., Formenti, P., Afif, C., Ancellet, G., Attié, J.-L., Bechara, J., Borbon, A., Cairo, F., Coe, H. and Crumeyrolle, S., 2010. Chemical and aerosol characterisation of the troposphere over West Africa during the monsoon period as part of AMMA. Atmospheric Chemistry and Physics, 10(16): 7575-7601.

Roiger, A., Thomas, J.-L., Schlager, H., Law, K.S., Kim, J., Schäfler, A., Weinzierl, B., Dahlkötter, F., Krisch, I. and Marelle, L., 2015. Quantifying emerging local anthropogenic emissions in the Arctic region: the ACCESS aircraft campaign experiment. bulletin of the american meteorological Society, 96(3): 441-460.

RTI, 2011. Emission protocol for petroleum refineries v 2.1.1, RTI International, Research Triangle Park, NC 27709-2194. http://www.epa.gov/ttnchie1/efpac/protocol/Emission_Estimation_Protocol_for_Petroleum_Refinerie_052011.pdf.

Schultz, C., 2014. Texas refinery air pollution emissions are being severely underestimated. Eos, Transactions American Geophysical Union, 95(24): 208-208.

Seinfeld, J., 2008. Atmospheric science: Black carbon and brown clouds. Nature geoscience, 1(1): 15-16.

Sivathanu, Y. and Faeth, G.M., 1990. Soot volume fractions in the overfire region of turbulent diffusion flames. Combustion and flame, 81(2): 133-149.

Smith, D. and Chughtai, A., 1995. The surface structure and reactivity of black carbon. Colloids and Surfaces A: Physicochemical and Engineering Aspects, 105(1): 47-77.

Sonibare, J., Adebiyi, F., Obanijesu, E. and Okelana, O., 2010. Air quality index pattern around petroleum production facilities. Management of Environmental Quality: An International Journal, 21(3): 379-392.

Sonibare, J.A. and Akeredolu, F.A., 2004. A theoretical prediction of non-methane gaseous emissions from natural gas combustion. Energy Policy, 32(14): 1653-1665.

Stocker, T., Qin, D., Plattner, G., Tignor, M., Allen, S., Boschung, J., Nauels, A., Xia, Y., Bex, B. and Midgley, B., 2013. IPCC, 2013: climate change 2013: the physical science basis. Contribution of working group I to the fifth assessment report of the intergovernmental panel on climate change.

Stohl, A., Klimont, Z., Eckhardt, S., Kupiainen, K., Shevchenko, V., Kopeikin, V. and Novigatsky, A., 2013. Black carbon in the Arctic: the underestimated role of gas flaring and residential combustion emissions. Atmospheric Chemistry and Physics, 13(17): 8833-8855.

Stone, D.K., Lynch, S.K., Pandullo, R.F., Evans, L.B. and Vatavuk, W.M., 1992. Flares. Part I: Flaring Technologies for Controlling VOC-Containing Waste Streams. Journal of the Air & Waste Management Association, 42(3): 333-340.

Strosher, M.T., 2000. Characterization of emissions from diffusion flare systems. Journal of the Air & Waste Management Association, 50(10): 1723-1733.

Sultan, B. and Janicot, S., 2003. The West African monsoon dynamics. Part II: The “preonset” and “onset” of the summer monsoon. Journal of climate, 16(21): 3407-3427.

Talebi, A., Fatehifar, E., Alizadeh, R. and Kahforoushan, D., 2014. The Estimation and Evaluation of New CO, CO2, and NOx Emission Factors for Gas Flares Using Pilot Scale Flare. Energy Sources, Part A: Recovery, Utilization, and Environmental Effects, 36(7): 719-726.

Tesner, P., Smegiriova, T. and Knorre, V., 1971a. Kinetics of dispersed carbon formation. Combustion and Flame, 17(2): 253-260.

Tesner, P., Tsygankova, E., Guilazetdinov, L., Zuyev, V. and Loshakova, G., 1971b. The formation of soot from aromatic hydrocarbons in diffusion flames of hydrocarbon-hydrogen mixtures. Combustion and Flame, 17(3): 279-285.

Torres, V.M., Herndon, S. and Allen, D.T., 2012a. Industrial flare performance at low flow conditions. 2. Steam-and air-assisted flares. Industrial & Engineering Chemistry Research, 51(39): 12569-12576.

Torres, V.M., Herndon, S., Kodesh, Z. and Allen, D.T., 2012b. Industrial flare performance at low flow conditions. 1. Study overview. Industrial & Engineering Chemistry Research, 51(39): 12559-12568.

Tripathi, S., Dey, S., Tare, V. and Satheesh, S., 2005. Aerosol black carbon radiative forcing at an industrial city in northern India. Geophysical Research Letters, 32(8).

Tumolva, L., Park, J.-Y., Kim, J.-s., Miller, A.L., Chow, J.C., Watson, J.G. and Park, K., 2010. Morphological and elemental classification of freshly emitted soot particles and atmospheric ultrafine particles using the TEM/EDS. Aerosol Science and Technology, 44(3): 202-215.

USEPA, 1995. AP 42-Compilation of air pollutant emission factors. Section 13.5: Industrial flares, U.S Environmental Protection Agenecy, Office of Air quality planning and standards, Research Triangle Park, NC. http://www.epa.gov/ttn/chief/ap42/ch13/final/c13s05.pdf.

USEPA, 2000. Test Method 5-Determination of particulate matter emissions from stationary sources, U.S Environmental Protection Agency. www.epa.gov/ttnemc01/methods/methods5.html.

USEPA, 2008. Direct emissions from stationary combustion sources EPA430-K-08-003, United States Environmental Protection Agency http://www.epa.gov/climateleadership/documents/resources/stationarycombustionguidance.pdf.

USEPA, 2010. Integrated Science Assessment for Particulate Matter, US Environmental Protection Agency, Washington, DC.

USEPA, 2011. Emission Estimation Protocol for Petroleum Refineries, US Environmental Protection Agency, Washington, DC.

USEPA, 2012. Report to congress on Black Carbon. EPA-450/R-12-001, United States Environmental Protection Agency, Research Triangle Park, NC.

USEPA, 2014. AP 42-Compilation of air pollutant emission factors. Section 13.5: Industrial flares

U.S Environmental Protection Agenecy, Office of Air quality planning and standards, Research Triangle Park, NC. http://www.epa.gov/ttn/chief/ap42/ch13/final/dc13s05_8-19-14.pdf.

Villasenor, R., Magdaleno, M., Quintanar, A., Gallardo, J., López, M., Jurado, R., Miranda, A., Aguilar, M., Melgarejo, L. and Palmerın, E., 2003. An air quality emission inventory of offshore operations for the exploration and production of petroleum by the Mexican oil industry. Atmospheric Environment, 37(26): 3713-3729.

Wang, X., Heald, C., Ridley, D., Schwarz, J., Spackman, J., Perring, A., Coe, H., Liu, D. and Clarke, A., 2014. Exploiting simultaneous observational constraints on mass and absorption to estimate the global direct radiative forcing of black carbon and brown carbon. Atmospheric Chemistry and Physics, 14(20): 10989-11010.

William, F., 1985. Combustion Theory: The fundamental theory of chemically reacting flow system. The Benjamin/Cummings Publishing Company, Menlo Park, CA.

Zhang, J.J. and Morawska, L., 2002. Combustion sources of particles: 2. Emission factors and measurement methods. Chemosphere, 49(9): 1059-1074.